Automatica 90 (2018) 172–184

Contents lists available at ScienceDirect

Automatica

journal homepage: www.elsevier.com/locate/automatica

Robust MPC for tracking constrained unicycle robots with additive disturbances ☆

Zhongqi Sun [a], Li Dai [a], Kun Liu [a], Yuanqing Xia [a,*], Karl Henrik Johansson [b]

[a] School of Automation, Beijing Institute of Technology, Beijing 100081, China
[b] School of Electrical Engineering, KTH Royal Institute of Technology, SE-100 44 Stockholm, Sweden

ARTICLE INFO

Article history:
Received 18 November 2016
Received in revised form 21 June 2017
Accepted 28 September 2017
Available online 15 February 2018

Keywords:
Robust control
Model predictive control (MPC)
Unicycle robots
Bounded disturbances

ABSTRACT

Two robust model predictive control (MPC) schemes are proposed for tracking unicycle robots with input constraint and bounded disturbances: tube-MPC and nominal robust MPC (NRMPC). In tube-MPC, the control signal consists of a control action and a nonlinear feedback law based on the deviation of the actual states from the states of a nominal system. It renders the actual trajectory within a tube centered along the optimal trajectory of the nominal system. Recursive feasibility and input-to-state stability are established and the constraints are ensured by tightening the input domain and the terminal region. In NRMPC, an optimal control sequence is obtained by solving an optimization problem based on the current state, and then the first portion of this sequence is applied to the real system in an open-loop manner during each sampling period. The state of the nominal system model is updated by the actual state at each step, which provides additional feedback. By introducing a robust state constraint and tightening the terminal region, recursive feasibility and input-to-state stability are guaranteed. Simulation results demonstrate the effectiveness of both strategies proposed.

1. Introduction

Tracking control of nonholonomic systems is a fundamental motion control problem and has broad applications in many important fields such as unmanned ground vehicle navigation (Simanek, Reinstein, & Kubelka, 2015), multi-vehicle cooperative control (Wang & Ding, 2014) and formation control (Lafferriere, Williams, Caughman, & Veerman, 2005). So far, many techniques have been developed for control of nonholonomic robots (Ghommam, Mehrjerdi, Saad, & Mnif, 2010; Jiang & Nijmeijer, 1997; Lee, Song, Lee, & Teng, 2001; Marshall, Broucke, & Francis, 2006; Yang & Kim, 1999). However, these techniques either ignore the mechanical constraints, or require the persistent excitation of the reference trajectory, i.e., the linear and angular velocity must not converge to zero (Gu & Hu, 2006). Model predictive control (MPC) is widely used for constrained systems. By solving a finite horizon open-loop optimization problem on-line based on the current system state at each sampling instant, an optimal control sequence is obtained. The first portion of the sequence is applied to the system at each actuator update (Mayne, Rawlings, Rao, & Scokaert, 2000). MPC of four-wheel vehicles was studied in Frasch et al. (2013), Shakouri and Ordys (2011, 2014) and Tashiro (2013), in which real-time control for application was emphasized. MPC for tracking of noholonomic systems was studied in Chen, Sun, Yang, and Chen (2010), Gu and Hu (2006), Sun and Xia (2016) and Wang and Ding (2014), where the robots were considered to be perfectly modeled. However, when the system is uncertain or perturbed, stability and feasibility of such MPC may be lost. Stochastic MPC and robust MPC are two main approaches to deal with uncertainty (Mayne, 2016). In stochastic MPC, it usually "soften" the state and terminal constraints to obtain a meaningful optimal control problem (see Dai, Xia, Gao, Kouvaritakis, & Cannon, 2015; Grammatico, Subbaraman, & Teel, 2013; Hokayem, Cinquemani, Chatterjee, Ramponi, & Lygeros, 2012; Zhang, Georghiou, & Lygeros, 2015). This paper focuses on robust MPC and will present two robust MPC schemes for a classical unicycle robot tracking problem.

There are several design methods for robust MPC. One of the simplest approaches is to ignore the uncertainties and rely on the inherent robustness of deterministic MPC, in which an open-loop control action computed on-line is applied recursively to the system (Marruedo, Alamo, & Camacho, 2002b; Scokaert & Rawlings,

☆ This work was supported in part by the Beijing Natural Science Foundation under Grant 4161001, in part by the National Natural Science Foundation of China under Grant 61720106010, Grant 61422102, Grant 61603041 and Grant 61503026, and in part by the Foundation for Innovative Research Groups of the National Natural Science Foundation of China under Grant 61621063. The material in this paper was not presented at any conference. This paper was recommended for publication in revised form by Associate Editor Riccardo Scattolini under the direction of Editor Ian R. Petersen.

* Corresponding author.
E-mail addresses: 0386@bit.edu.cn (Z. Sun), li.dai@bit.edu.cn (L. Dai), kunliubit@bit.edu.cn (K. Liu), xia_yuanqing@bit.edu.cn (Y. Xia), kallej@kth.se (K.H. Johansson).

https://doi.org/10.1016/j.automatica.2017.12.048
0005-1098/

1995). However, the open-loop control and the uncertainty may degrade the control performance, or even render the system unstable. Hence, feedback MPC was proposed in Kothare, Balakrishnan, and Morari (1996), Lee and Yu (1997) and Wan and Kothare (2002), in which a sequence of feedback control laws is obtained by solving an optimization problem. The determination of a feedback policy is usually prohibitively difficult. To overcome this difficulty, it is intuitive to focus on simplifying approximations by, for instance, solving a min–max optimization problem on-line. Min–max MPC provides a conservative robust solution for systems with bounded disturbances by considering all possible disturbances realizations (Lee & Yu, 1997; Limón, Alamo, Salas, & Camacho, 2006; Wan & Kothare, 2002). It is in most cases computationally intractable to achieve such feedback laws, since the computational complexity of min–max MPC grows exponentially with the increase of the prediction horizon.

Tube-MPC taking advantage of both open-loop and feedback MPC approaches was reported in Fleming, Kouvaritakis, and Cannon (2015), Langson, Chryssochoos, Raković, and Mayne (2004), Mayne, Kerrigan, Van Wyk, and Falugi (2011), Mayne and Langson (2001), Mayne, Seron, and Raković (2005) and Yu, Maier, Chen, and Allgöwer (2013). Here the controller consists of an optimal control action and a feedback control law. The optimal control action steers the state to the origin asymptotically, and the feedback control law maintains the actual state within a "tube" centered along the optimal state trajectory. Tube-MPC for linear systems was advocated in Langson et al. (2004) and Mayne and Langson (2001), where the center of the tube was provided by employing a nominal system and the actual trajectory was restricted by an affine feedback law. It was shown that the computational complexity is linear rather than exponential with the increase of prediction horizon. The authors of Mayne et al. (2005) took the initial state of the nominal system employed in the optimization problem as a decision variable in addition to the traditional control sequence, and proved several potential advantages of such an approach. Tube-MPC for nonlinear systems with additive disturbances was studied in Mayne et al. (2011) and Yu et al. (2013), where the controller possessed a similar structure as in the linear case but the feedback law was replaced by another MPC to attenuate the effect of disturbances. Two optimization problems have to be solved on-line, which increases the computation burden.

In fact, tube-MPC provides a suboptimal solution because it has to tighten the input domain in the optimization problem, which may degrade the control performance. It is natural to inquire if nominal MPC is sufficiently robust to disturbances. A robust MPC via constraint restriction was developed in Chisci, Rossiter, and Zappa (2001) for discrete-time linear systems, in which asymptotic state regulation and feasibility of the optimization problem were guaranteed. In Marruedo, Alamo, and Camacho (2002a), a robust MPC for discrete-time nonlinear systems using nominal predictions was presented. By tightening the state constraints and choosing a suitable terminal region, robust feasibility and input-to-state stability were guaranteed. In Richards and How (2006), the authors designed a constraint tightened in a monotonic sequence in the optimization problem such that the solution is feasible for all admissible disturbances. A novel robust dual-mode MPC scheme for a class of nonlinear systems was proposed in Li and Shi (2014b), the system of which is assumed to be linearizable. Since the procedure of this class of robust MPC is almost the same as nominal MPC, we call this class nominal robust MPC (NRMPC) in this paper.

Robust MPC for linear systems is well studied but for nonlinear systems is still challenging since it is usually intractable to design a feedback law yielding a corresponding robust invariant set. Especially, the study of robust MPC for nonholonomic systems remains open. Consequently, this paper focuses on the design of robust MPC for the tracking of unicycle robots with coupled input constraint and bounded additive disturbance, which represents a particular class of nonholonomic systems. We discuss the two robust MPC schemes introduced above. First, a tube-MPC strategy with two degrees of freedom is developed, in which the nominal system is employed to generate a central trajectory and a nonlinear feedback is designed to steer the system trajectory within the tube for all admissible disturbances. Recursive feasibility and input-to-state stability are guaranteed by tightening the input domain and terminal constraint via affine transformation and all the constraints are ensured. Since tube-MPC sacrifices optimality for simplicity, an NRMPC strategy is presented, in which the state of the nominal system is updated by the actual one in each step. In such a way, the control action applied to the real system is optimal with respect to the current state. Input-to-state stability is also established in this case by utilizing the recursive feasibility and the tightened terminal region.

The remainder of this paper is organized as follows. In Section 2, we outline the control problem and some preliminaries. Tube-MPC and NRMPC are developed in Sections 3 and 4, respectively. In Section 5, simulation results are given. Finally, we summarize the paper in Section 6.

Notation: $\mathbb{R}$ denotes the real space and $\mathbb{N}$ denotes the collection of all nonnegative integers. For a given matrix M, $\|M\|$ denotes its 2-norm. $\text{diag}\{x_1, x_2, \ldots, x_n\}$ denotes the diagonal matrix with entries $x_1, x_2, \ldots, x_n \in \mathbb{R}$. For two vectors $x = [x_1, x_2, \ldots, x_n]^{\mathrm{T}}$ and $y = [y_1, y_2, \ldots, y_n]^{\mathrm{T}}$, $x < y$ means $\{x_1 < y_1, x_2 < y_2, \ldots, x_n < y_n\}$ and $|x| \triangleq [|x_1|, |x_2|, \ldots, |x_n|]^{\mathrm{T}}$ denotes its absolute value. $\|x\| \triangleq \sqrt{x^{\mathrm{T}}x}$ is the Euclidean norm. P-weighted norm is denoted as $\|x\|_P \triangleq \sqrt{x^{\mathrm{T}}Px}$, where P is a positive definite matrix with appropriate dimension. Given two sets $\mathbb{A}$ and $\mathbb{B}$, $\mathbb{A} \oplus \mathbb{B} \triangleq \{a + b | a \in \mathbb{A}, b \in \mathbb{B}\}$, $\mathbb{A} \ominus \mathbb{B} \triangleq \{a | \{a\} \oplus \mathbb{B} \subset \mathbb{A}\}$ and $M\mathbb{A} \triangleq \{Ma | a \in \mathbb{A}\}$, where M is a matrix with appropriate dimensions.

2. Problem formulation and preliminaries

In this section, we first introduce the kinematics of the nonholonomic robot and deduce the coupled input constraint from its mechanical model. Then, we formulate the tracking problem as our control objective, and finally give some preliminaries for facilitating the development of our main results.

2.1. Kinematics of the unicycle robot

Consider a nonholonomic robot described by the following unicycle-modeled kinematics:

$$\dot{\xi}(t) = f(\xi(t), u(t)) = \begin{bmatrix} \cos\theta(t) & 0 \\ \sin\theta(t) & 0 \\ 0 & 1 \end{bmatrix} u(t), \tag{1}$$

where $\xi(t) = [p^{\mathrm{T}}(t), \theta(t)]^{\mathrm{T}} \in \mathbb{R}^2 \times (-\pi, \pi]$ is the state, consisting of position $p(t) = [x(t), y(t)]^{\mathrm{T}}$ and orientation $\theta(t)$, and $u(t) = [v(t), \omega(t)]^{\mathrm{T}}$ is the control input with the linear velocity $v(t)$ and the angular velocity $\omega(t)$.

The unicycle robot is shown in Fig. 1, where $\rho > 0$ is half of the wheelbase, v^L and v^R are the velocities of the left and the right driving wheels, respectively. It is assumed that the two wheels possess the same mechanical properties and the magnitudes of their velocities are bounded by $|v^L| \leq a$ and $|v^R| \leq a$, where $a \in \mathbb{R}$ is a known positive constant. The linear and angular velocities of the robot are then

$$\begin{aligned} v &= (v^L + v^R)/2, \\ \omega &= (v^R - v^L)/2\rho. \end{aligned} \tag{2}$$

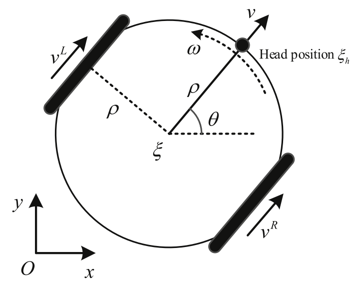

Fig. 1. Unicycle robot.

As a consequence, the control input u should be bounded by the set

$$\mathbb{U} = \{[v, \omega]^{\mathrm{T}} : \frac{|v|}{a} + \frac{|\omega|}{b} \leq 1\} \tag{3}$$

with $b = a/\rho$, i.e., $u \in \mathbb{U}$.

2.2. Control objective

Our control objective is to track a reference trajectory using separation-bearing control (Das et al., 2002; Desai, Ostrowski, & Kumar, 2001). We formulate this problem in a relative coordinate system. The reference trajectory, which can be viewed as a virtual leader, is described by a reference state vector $\xi_r(t) = [p_r^{\mathrm{T}}(t), \theta_r(t)]^{\mathrm{T}} \in \mathbb{R}^2 \times (-\pi, \pi]$ with $p_r(t) = [x_r(t), y_r(t)]^{\mathrm{T}}$ and a reference control signal $u_r(t) = [v_r(t), \omega_r(t)] \in \mathbb{U}$. The reference state vector $\xi_r(t)$ and the reference control signal $u_r(t)$ are modeled as a nominal unicycle robot

$$\dot{\xi}_r(t) = f(\xi_r(t), u_r(t)). \tag{4}$$

The robot to be controlled is defined as a follower and is also a unicycle with kinematics (1). As the existence of nonholonomic constraint, we consider its head position, which is the point that lies a distance ρ along the perpendicular bisector of the wheel axis ahead of the robot. Furthermore, the robot is assumed to be perturbed by a disturbance caused by sideslip due to the road ride. Therefore, we consider disturbances acting on the linear velocity while neglecting disturbances acting on the angular velocity. The perturbed head position kinematics is then formulated as follows:

$$\dot{\xi}_f(t) = f_h(\xi_f(t), u_f(t)) + d(t), \quad u_f(t) \in \mathbb{U}, \tag{5}$$

where $\xi_f(t) = [p_f^{\mathrm{T}}(t), \theta_f(t)]^{\mathrm{T}}$ is the state with head position $p_f(t) = [x_f(t), y_f(t)]^{\mathrm{T}}$, and $u_f(t) = [v_f(t), \omega_f(t)]^{\mathrm{T}}$ is the control input. Here, the nonlinear function f_h is given by $f_h(\xi_f(t), u_f(t)) = [(M(\theta_f(t))u_f(t))^{\mathrm{T}}, \omega_f(t)]^{\mathrm{T}}$ with $M(\theta_f) = \begin{bmatrix} \cos\theta_f & -\rho\sin\theta_f \\ \sin\theta_f & \rho\cos\theta_f \end{bmatrix}$. In addition, $d(t) = [d_p^{\mathrm{T}}(t), 0]^{\mathrm{T}} \subseteq \mathbb{R}^3$ with $d_p(t) = [d_x(t), d_y(t)]^{\mathrm{T}}$ is the external disturbances, which is bounded by

$$\|d(t)\| \leq \eta. \tag{6}$$

Construct Frenet–Serret frames ${}^rO$ and ${}^fO$ for the virtual leader and the follower, respectively. They are moving coordinate systems fixed on the robots (see Fig. 2). The desired position is $p_d = [x_d, y_d]^{\mathrm{T}}$, which is defined with respect to the Frenet–Serret frame ${}^rO$. At the same time, the tracking error $p_e = [x_e, y_e]^{\mathrm{T}}$ is defined with respect to the Frenet–Serret frame ${}^fO$ and is given by

$$p_e(t) = R(-\theta_f(t))(p_r(t) - p_f(t)) + R(\theta_e)p_d, \tag{7}$$

$$\theta_e(t) = \theta_r(t) - \theta_f(t), \tag{8}$$

where $R(\theta) = \begin{bmatrix} \cos\theta & -\sin\theta \\ \sin\theta & \cos\theta \end{bmatrix}$ is the rotation matrix.

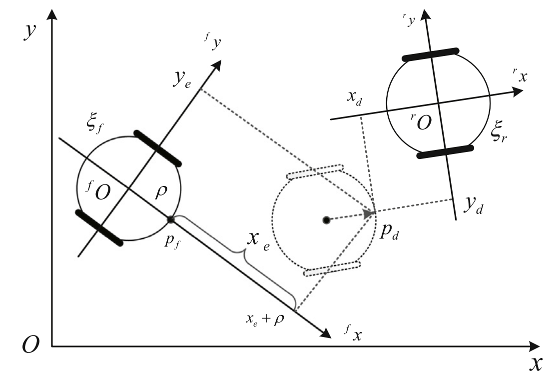

Fig. 2. Leader–follower configuration.

Taking the derivative of the tracking error yields

$$\dot{p}_e(t) = \begin{bmatrix} 0 & \omega_f \\ -\omega_f & 0 \end{bmatrix} \begin{bmatrix} x_e \\ y_e \end{bmatrix} + \begin{bmatrix} -v_f + (v_r - x_d\omega_r)\cos\theta_e - x_d\omega_r\sin\theta_e \\ -\rho\omega_f + (v_r - x_d\omega_r)\sin\theta_e + y_d\omega_r\cos\theta_e \end{bmatrix} + R(\theta_f)d_p. \tag{9}$$

We will design robust MPC strategies to drive the tracking error p_e to a neighborhood of the origin. Note that the tracking system (9) involves the disturbances but the future disturbances cannot be predicted in advance. We will formulate the MPC problem only involving the nominal system.

To distinguish the variables in the nominal system model from the real system, we introduce $\tilde{\cdot}$ as a superscript for the variables in the nominal system. From the perturbed system (5), the nominal dynamics can be obtained by neglecting the disturbances as

$$\dot{\tilde{\xi}}_f(t) = f_h(\tilde{\xi}_f(t), \tilde{u}_f(t)), \quad \tilde{u}_f(t) \in \mathbb{U}, \tag{10}$$

where, similarly, $\tilde{\xi}_f(t) = [\tilde{p}_f^{\mathrm{T}}(t), \tilde{\theta}_f(t)]^{\mathrm{T}}$ is the state of the nominal system with the position $\tilde{p}_f = [\tilde{x}_f(t), \tilde{y}_f(t)]^{\mathrm{T}}$ and orientation $\tilde{\theta}_f(t)$, and $\tilde{u}_f(t) = [\tilde{v}_f(t), \tilde{\omega}_f(t)]^{\mathrm{T}}$ is the control input of the nominal system. The tracking error dynamics based on the nominal system is then given by

$$\dot{\tilde{p}}_e(t) = \begin{bmatrix} 0 & \omega_f(t) \\ -\omega_f(t) & 0 \end{bmatrix} \begin{bmatrix} \tilde{x}_e(t) \\ \tilde{y}_e(t) \end{bmatrix} + \tilde{u}_e(t), \tag{11}$$

where $\tilde{u}_e(t)$ is the input error and is given by

$$\tilde{u}_e(t) = \begin{bmatrix} -\tilde{v}_f + (v_r - x_d\omega_r)\cos\tilde{\theta}_e - x_d\omega_r\sin\tilde{\theta}_e \\ -\rho\tilde{\omega}_f + (v_r - x_d\omega_r)\sin\tilde{\theta}_e + y_d\omega_r\cos\tilde{\theta}_e \end{bmatrix}.$$

Define $\{t_k : k \in \mathbb{N}, t_{k+1} - t_k = \delta\}$, with $\delta > 0$, as the time sequence at which the open-loop optimization problems are solved. The MPC cost to be minimized is given by

$$J(\tilde{p}_e(t_k), \tilde{u}_e(t_k)) = \int_{t_k}^{t_k+T} L(\tilde{p}_e(\tau|t_k), \tilde{u}_e(\tau|t_k))d\tau + g(\tilde{p}_e(t_k+T|t_k)), \tag{12}$$

in which $L(\tilde{p}_e(\tau|t_k), \tilde{u}_e(\tau|t_k)) = \|\tilde{p}_e(\tau|t_k)\|_Q^2 + \|\tilde{u}_e(\tau|t_k)\|_P^2$ represents the stage cost with the positive definite matrices $P = \mathrm{diag}\{p_1, p_2\}$ and $Q = \mathrm{diag}\{q_1, q_2\}$, $g(\tilde{p}_e(\tau|t_k)) = \frac{1}{2}\|\tilde{p}_e(\tau|t_k)\|^2$ is the terminal penalty, and T is the prediction horizon satisfying $T = N\delta$, $N \in \mathbb{N}$.

2.3. Preliminaries

Some definitions and lemmas used in the following sections are summarized as follows.

Definition 1. For the nominal tracking error system (11), the terminal region Ω and the terminal controller $\tilde{u}_f^\kappa(\cdot)$ are such that if $\tilde{p}_e(t_k+T|t_k) \in \Omega$, then, for any $\tau \in (t_k+T, t_{k+1}+T]$, by implementing the terminal controller $\tilde{u}_f(\tau|t_{k+1}) = \tilde{u}_f^\kappa(\tau|t_{k+1})$, it holds that

$$\tilde{p}_e(\tau|t_k) \in \Omega, \tag{13}$$

$$\tilde{u}_f(\tau|t_k) \in \mathbb{U}, \tag{14}$$

$$\dot{g}(\tilde{p}_e(\tau|t_k)) + L(\tilde{p}_e(\tau|t_k), \tilde{u}_e(\tau|t_k)) \le 0. \tag{15}$$

Definition 2 (Sontag, 2008)**.** System (9) is input-to-state stable (ISS) if there exist a $\mathcal{KL}$ function $\beta(\cdot,\cdot) : \mathbb{R}_{\ge 0} \times \mathbb{R}_{\ge 0} \to \mathbb{R}$ and a $\mathcal{K}$ function $\gamma(\cdot)$ such that, for $t \ge 0$, it holds that

$$\|p_e(t)\| \le \beta(\|p_e(t_0)\|, t) + \gamma(\eta), \tag{16}$$

where t_0 is the initial time and η is the bound of disturbance given by (6).

Definition 3 (Sontag, 2008)**.** A function $V(\cdot)$ is called an ISS-Lyapunov function for system (9) if there exist $\mathcal{K}_\infty$ functions $\alpha_1(\cdot)$, $\alpha_2(\cdot)$, $\alpha_3(\cdot)$ and a $\mathcal{K}$ function $\sigma(\cdot)$ such that for all $p_e \in \mathbb{R}^2$

$$\alpha_1(\|p_e(t_k)\|) \le V(p_e(t_k)) \le \alpha_2(\|p_e(t_k)\|), \tag{17}$$

$$V(p_e(t_{k+1})) - V(p_e(t_k)) \le -\alpha_3(\|p_e(t_k)\|) + \sigma(\eta), \tag{18}$$

where η is the bound of the disturbance given by (6).

Remark 1. If Definition 2 or 3 holds, then it implies that the tracking error vanishes if there is no disturbance.

The following lemma provides a terminal controller and the corresponding terminal region for the nominal error system (11).

Lemma 1. *For the nominal tracking system (11), let $\tilde{u}_f \in \lambda_f \mathbb{U}$ with $\lambda_f \in (0, 1]$, $\|u_r\| < \frac{a}{\sqrt{2}\|D\|}\lambda_f$ with $D = \begin{bmatrix} 1 & -x_d \\ 0 & y_d \end{bmatrix}$, and $\lambda_r = \frac{\sqrt{2}\|D\|}{a} \max \|u_r\|$. Then $\Omega = \{\tilde{p}_e : \tilde{k}_1|\tilde{x}_e| + \tilde{k}_2|\tilde{y}_e| < a(\lambda_f - \lambda_r)\}$ is a terminal region for the controller*

$$\tilde{u}_f^\kappa(\tau|t_k) = \begin{bmatrix} \tilde{k}_1\tilde{x}_e + (v_r - x_d\omega_r)\cos\tilde{\theta}_e - x_d\omega_r \sin\tilde{\theta}_e \\ \dfrac{1}{\rho}(\tilde{k}_2\tilde{y}_e + (v_r - x_d\omega_r)\sin\tilde{\theta}_e + y_d\omega_r\cos\tilde{\theta}_e) \end{bmatrix},$$
$$\tau \in [t_k+T, t_{k+1}+T), \tag{19}$$

with the parameters satisfying $p_iq_i < \frac{1}{4}$ and $\tilde{k}_i \in \left(\frac{1-\sqrt{1-4p_iq_i}}{2p_i}, \frac{1+\sqrt{1-4p_iq_i}}{2p_i}\right)$, $i = 1, 2$. Here, p_i and q_i are the entries of P and Q, respectively, given by (12).

The proof of Lemma 1 is provided in Appendix.

Nominal system (10) is Lipschitz continuous and a corresponding Lipschitz constant is given by the following lemma (see Appendix for the detailed proof).

Lemma 2. *System (10) with $u \in \mathbb{U}$ is locally Lipschitz in ξ with Lipschitz constant a, where a is the max wheel speed.*

3. Tube-MPC

In this section, a tube-MPC policy is developed. It consists of an optimal control action obtained by solving an optimization problem and a feedback law based on the deviation of the actual state from the nominal one. The controller forces the system state to stay within a tube around a sensible central trajectory. The central trajectory is determined by the following optimization problem.

Problem 1.

$$\min_{\tilde{u}_f(\tau|t_k)} \quad J(\tilde{p}_e(t_k), \tilde{u}_e(t_k)), \tag{20}$$

$$s.t. \quad p_f(t_k) \in \tilde{p}_f(t_k|t_k) \oplus \mathbb{P}_{fe}, \tag{21}$$

$$\dot{\tilde{\xi}}_f(\tau|t_k) = f_h(\tilde{\xi}_f(\tau|t_k), \tilde{u}_f(\tau|t_k)), \tag{22}$$

$$\tilde{u}_f(\tau|t_k) \in \mathbb{U}_{\text{tube}}, \tag{23}$$

$$\tilde{p}_e(t_k+T|t_k) \in \Omega_{\text{tube}}, \tag{24}$$

where $\mathbb{P}_{fe} = \left\{p_{fe}(t) : |p_{fe}| \le [-\frac{\eta}{k_1}, -\frac{\eta}{k_2}]^{\mathrm{T}}\right\}$, $\mathbb{U}_{\text{tube}} = \{[\tilde{v}_f, \tilde{\omega}_f]^{\mathrm{T}} : \frac{|\tilde{v}_f|}{a} + \frac{|\tilde{\omega}_f|}{b} \le \lambda_{\text{tube}}\}$ with $\lambda_{\text{tube}} = \frac{\sqrt{2}}{2} - \frac{\eta\sqrt{2}}{a}$, and $\Omega_{\text{tube}} = \{\tilde{p}_e : \tilde{k}_1|\tilde{x}_e| + \tilde{k}_2|\tilde{y}_e| < a(\lambda_{\text{tube}} - \lambda_r)\}$.

Remark 2. Problem 1 is a nonlinear programming problem. Numerical solutions can be found by several algorithms, such as interior point method (Wächter & Biegler, 2006), trust region reflective algorithm (Coleman & Li, 1996), branch-and-bound optimization (Narendra & Fukunaga, 1977), etc.

Solution of Problem 1 yields the minimizing control sequence for the nominal follower system over the interval $[t_k, t_k+T)$:

$$\tilde{\boldsymbol{u}}_f^*(t_k) = \left\{\tilde{u}_f^*(\tau|t_k) : \tau \in [t_k, t_k+T)\right\}, \tag{25}$$

as well as the corresponding optimal trajectory:

$$\tilde{\boldsymbol{\xi}}_f^*(t_k) = \left\{[\tilde{p}_f^{*\mathrm{T}}(\tau|t_k), \tilde{\theta}_f^*(\tau|t_k)]^{\mathrm{T}} : \tau \in [t_k, t_k+T)\right\}. \tag{26}$$

Applying the control in (25), for $t \in [t_k, t_{k+1})$, to the actual system may not drive the state along the optimal trajectory (26) due to the external disturbance. We denote the deviation of the actual trajectory from the optimal trajectory as

$$p_{fe}(t) = p_f(t) - \tilde{p}_f^*(t|t_k). \tag{27}$$

Taking the derivative of (27) yields

$$\dot{p}_{fe}(t) = M(\theta_f(t))u_f(t) - M(\tilde{\theta}_f^*(t|t_k))\tilde{u}_f^*(t|t_k) + d_p(t). \tag{28}$$

The robust controller for the follower over the interval $t \in [t_k, t_{k+1})$ is then

$$u_f(t) = M^{-1}(\theta_f(t))[M(\tilde{\theta}_f^*(t|t_k))\tilde{u}_f^*(t|t_k) + Kp_{fe}(t)], \tag{29}$$

where $K = \mathrm{diag}\{k_1, k_2\}$, $k_1 < 0$ and $k_2 < 0$, is the feedback gain, $\tilde{u}_f^*(\tau|t_k)$, $\tilde{p}_f^*(\tau|t_k)$ and $\tilde{\theta}_f^*(\tau|t_k)$, $\tau \in [t_k, t_{k+1})$, are the first portion of the optimal control, trajectory and orientation, respectively, and $M(\theta)$ is given in (5).

Remark 3. Due to the system nonlinearity, the optimal control signal and the feedback law are different here compared to linear systems (Langson et al., 2004; Mayne & Langson, 2001; Mayne et al., 2005), in which the controllers have the form $u = u^* + K(x - x^*)$. The control in (29) is derived by feedback linearization of (28). The scheme leads to challenges in determining the tightened input constraint set $\mathbb{U}_{\text{tube}}$ such that $u_f \in \mathbb{U}$ holds. The scheme is also different from existing works on nonlinear systems as in Gao, Gray, Carvalho, Tseng, and Borrelli (2014), Gao, Gray, Tseng, and Borrelli (2014), Mayne et al. (2011) and Yu et al. (2013). Our off-line feedback law is replaced with an online computation of another MPC in Mayne et al. (2011) and Yu et al. (2013), which increases the online computational burden. In Gao, Gray, Carvalho, et al. (2014) and Gao, Gray, Tseng, et al. (2014), the authors take the nonlinear part of the system and the external disturbance as a total uncertainty to design feedback laws, which is similar to the case of linear systems, but feasibility cannot be guaranteed.

Based on this control strategy, the procedure of tube-MPC is summarized in Algorithm 1.

Algorithm 1 Tube-MPC

1: At time t_k, measure the actual system state $p_f(t_k)$ and establish the initial condition $p_f(t_k) \in \tilde{p}_f(t_k|t_k) \oplus \mathbb{P}_{fe}$.
2: Solve Problem 1 based on nominal system to obtain the optimal control sequence $\tilde{\boldsymbol{u}}_f^*(t_k) = \arg\min_{u_f(\tau|t_k)} J_f(\tilde{p}_e(t_k), \tilde{u}_e(t_k))$.
3: Calculate the control signal $u_f(t) = M^{-1}(\theta_f(t))[M(\tilde{\theta}_f^*(t|t_k))\tilde{u}_f^*(t|t_k) + Kp_{fe}(t)]$, $t \in [t_k, t_{k+1})$.
4: Apply $u_f(t)$ to the real system during the sampling interval $[t_k, t_{k+1})$.
5: Update the time instant $t_k \to t_{k+1}$ and go to step 1.

Remark 4. Since the optimization problem is solved on-line at each step and the first optimal control action is employed to generate the control policy together with the feedback law, the computational complexity is determined by the nominal system. Hence, the scheme has the same computational complexity as the deterministic MPC.

Remark 5. The initial state $\tilde{p}_f(t_k)$ in (21) of Problem 1 is taken as a decision variable in addition to the usual control sequence. This idea is inspired by Langson et al. (2004) and Mayne et al. (2005). Constraint (21) can also be replaced by $\tilde{\xi}_f(t_k|t_k) = \tilde{\xi}_f(t_k)$ (see Gao, Gray, Tseng, et al., 2014; Mayne & Langson, 2001; Rawlings & Mayne, 2009; Yu et al., 2013), which would imply that the optimization problem employs only the nominal system and thus the predictive optimal trajectory would be independent of the actual state except for the initial one. The central trajectory of the tube can be calculated in a parallel or even off-line way if the initial state is known a priori.

Before stating the main results of tube-MPC, the following lemma is given to show that the feedback law renders the difference between the minimizing and actual trajectories bounded while guaranteeing the satisfaction of the input constraint.

Lemma 3. *For the tracking control system (9) with controller (29), it follows that*

(i) *the state of the real system lies in the tube $\mathbb{T} = \tilde{p}_f^* \oplus \mathbb{P}_{fe}$, where $\mathbb{P}_{fe}$ is given in Problem 1;*
(ii) *the input constraint is satisfied, i.e., $u_f \in \mathbb{U}$.*

Proof. Substituting (29) into (28), we can conclude that

$$\dot{p}_{fe}(t) = Kp_{fe}(t) + d_p(t), \tag{30}$$

of which the solution is given by

$$p_{fe}(t) = e^{Kt}p_{fe}(0) + \int_0^t e^{K(t-\tau)}d_p(\tau)d\tau. \tag{31}$$

By the initialization condition (21) and upper-bound of the disturbances, it follows that

$$|p_{fe}(t)| \leq \eta \begin{bmatrix} \frac{1}{k_1}e^{k_1 t} - \frac{1}{k_1} \\ \frac{1}{k_2}e^{k_2 t} - \frac{1}{k_2} \end{bmatrix}. \tag{32}$$

Consequently, $p_{fe}(t) \in \mathbb{P}_{fe}(t)$, where the set $\mathbb{P}_{fe}(t)$ is defined by

$$\mathbb{P}_{fe}(t) = \left\{ p_{fe}(t) : |p_{fe}(t)| \leq \eta \begin{bmatrix} \frac{1}{k_1}e^{k_1 t} - \frac{1}{k_1} \\ \frac{1}{k_2}e^{k_2 t} - \frac{1}{k_2} \end{bmatrix} \right\}. \tag{33}$$

Then $\mathbb{P}_{fe}$ can be given by

$$\mathbb{P}_{fe} = \lim_{t\to\infty} \mathbb{P}_{fe}(t) = \left\{ p_{fe}(t) : |p_{fe}| \leq \begin{bmatrix} -\frac{\eta}{k_1} \\ -\frac{\eta}{k_2} \end{bmatrix} \right\}. \tag{34}$$

From (27) and $p_{fe} \in \mathbb{P}_{fe}$, we have

$$p_f \in \tilde{p}_f^* \oplus \mathbb{P}_{fe}, \tag{35}$$

i.e., the trajectory lies in the tube $\mathbb{T}$.

For (ii), redefine the control input as

$$u_f^a = M(\theta_f)u_f, \tag{36}$$

$$u_f^{a*} = M(\tilde{\theta}_f^*)\tilde{u}_f^*. \tag{37}$$

It can be observed that $M(\cdot)$ is an affine transformation, which is equivalent to scaling ω_f ($\tilde{\omega}_f^*$) by ρ and rotate u_f ($\tilde{u}_f^*$) by θ_f ($\tilde{\theta}_f^*$). Thus, to prove $u_f \in \mathbb{U}$ if $u_f^* \in \mathbb{U}_{\text{tube}}$ is equivalent to show $u_f^a \in \mathbb{U}^a(\theta_f)$ if $u_f^{a*} \in \mathbb{U}_{\text{tube}}^a$ for every admissible θ_f and θ_f^*. The sets $\mathbb{U}^a(\theta_f)$ and $\mathbb{U}_{\text{tube}}^a(\tilde{\theta}_f^*)$ are defined as follows:

$$\mathbb{U}^a(\theta_f) = M(\theta_f)\{[v, \omega]^{\mathrm{T}} : \frac{|v|}{a} + \frac{|\omega|}{b} \leq 1\}, \tag{38}$$

$$\mathbb{U}_{\text{tube}}^a(\tilde{\theta}_f^*) = M(\tilde{\theta}_f^*)\{[v, \omega]^{\mathrm{T}} : \frac{|v|}{a} + \frac{|\omega|}{b} \leq \lambda_{\text{tube}}\}. \tag{39}$$

Substituting (36) and (37) into (29) yields

$$u_f^a = u_f^{a*} + Kp_{fe}. \tag{40}$$

It is obvious that

$$\bigcap_{\theta_f\in(-\pi,\pi]} \mathbb{U}^a(\theta_f) = \{[v, \omega]^{\mathrm{T}} : \|[v, \omega]^{\mathrm{T}}\| \leq a\frac{\sqrt{2}}{2}\}, \tag{41}$$

$$\bigcup_{\theta_f^*\in(-\pi,\pi]} \mathbb{U}_{\text{tube}}^a(\tilde{\theta}_f^*) = \{[v, \omega]^{\mathrm{T}} : \|[v, \omega]^{\mathrm{T}}\| \leq a\lambda_{\text{tube}}\}, \tag{42}$$

$$\begin{aligned} K\mathbb{P}_{fe} &= \left\{ Kp_{fe}(t) : |Kp_{fe}| \leq \begin{bmatrix} \eta \\ \eta \end{bmatrix} \right\} \\ &\subset \left\{ Kp_{fe}(t) : \|Kp_{fe}\| \leq \sqrt{2}\eta \right\}. \end{aligned} \tag{43}$$

Thus, it can be obtained that

$$\bigcup_{\theta_f^*\in(-\pi,\pi]} \mathbb{U}_{\text{tube}}^a \oplus K\mathbb{P}_{fe} \subset \bigcap_{\theta_f\in(-\pi,\pi]} \mathbb{U}^a, \tag{44}$$

which implies that $u_f^a \in \mathbb{U}^a$ holds for every admissible θ_f and $\tilde{\theta}_f^*$, and thus $u_f \in \mathbb{U}$ naturally holds. □

Remark 6. Note that the input domain is independent of the feedback gain K, which differs from the results of linear systems in Chisci et al. (2001), Langson et al. (2004) and Mayne and Langson (2001). Meanwhile, from (i) in Lemma 3, increasing K will reduce the difference between the actual trajectory and the optimal one, and consequently reduce the size of tube $\mathbb{T}$. It indicates that the steady state tracking performance could be enhanced by tuning K.

The main results of tube-MPC are given in the following theorem.

Theorem 1. *For the tracking control system (9) under Algorithm 1, if Problem 1 is feasible at time t_0, then,*

(i) *Problem 1 is feasible for all $t > t_0$;*
(ii) *the tracking control system (9) is ISS.*

Proof. From Lemma 1, Ω_{tube} is a terminal region by letting $\lambda_f = \lambda_{\text{tube}}$. We assume that a feasible solution exists and an optimal solution $\tilde{u}_f^*(t_k)$ is found at the sampling instant t_k. When applying this sequence to the nominal system, the tracking error of the nominal system is driven into the terminal region Ω_{tube}, i.e., $\tilde{p}_e^*(t_k + T|t_k) \in \Omega_{\text{tube}}$, along the corresponding open-loop trajectory $\tilde{\xi}_f^*(t_k)$ over $[t_k, t_k+T)$. In terms of Algorithm 1, the control (29) over $[t_k, t_{k+1})$ is applied to the actual system, and its state measurement at time t_{k+1} satisfies $p_f(t_{k+1}) \in \tilde{p}_f^*(t_{k+1}|t_k) \oplus \mathbb{P}_{fe}$. This implies that $\tilde{p}_f^*(t_{k+1}|t_k)$ is a feasible initial state for Problem 1. Therefore, to solve the open-loop optimization problem at t_{k+1} with this initial condition, a feasible control sequence can be constructed by

$$\tilde{u}_f(\tau|t_{k+1}) = \begin{cases} \tilde{u}_f^*(\tau|t_k), & \tau \in [t_{k+1}, t_k+T), \\ \tilde{u}_f^\kappa(\tau|t_k), & \tau \in [t_k+T, t_{k+1}+T), \end{cases} \tag{45}$$

where $\tilde{u}_f^\kappa(\tau|t_k)$ is the terminal controller given by (19). Since the terminal region Ω_{tube} is invariant with the control $\tilde{u}_f^\kappa(\tau|t_k)$, $\tilde{p}_e^*(t_k + T|t_k) \in \Omega_{\text{tube}}$ implies $\tilde{p}_e(t_{k+1}+T|t_{k+1}) \in \Omega_{\text{tube}}$. Then, result (i) can be achieved by induction.

For (ii), we first prove that the tracking error for the nominal system converges to the origin. Then we show that the state of the real system converges to an invariant set along a trajectory lying in the tube $\mathbb{T}$, the center of which is the trajectory of the nominal system. The Lyapunov function for the nominal system is chosen as

$$V(t_k) = J(\tilde{p}_e^*(t_k), \tilde{u}_e^*(t_k)). \tag{46}$$

Consider the difference of the Lyapunov function at t_k and t_{k+1},

$$\begin{aligned} \Delta V &= V(t_{k+1}) - V(t_k) \\ &\le J(\tilde{p}_e(t_{k+1}), \tilde{u}_e(t_{k+1})) - J(\tilde{p}_e^*(t_k), \tilde{u}_e^*(t_k)) \\ &= \int_{t_{k+1}}^{t_{k+1}+T} (\|\tilde{p}_e(\tau|t_{k+1})\|_Q^2 + \|\tilde{u}_e(\tau|t_{k+1})\|_P^2) d\tau \\ &\quad - \int_{t_k}^{t_k+T} (\|\tilde{p}_e^*(\tau|t_k)\|_Q^2 + \|\tilde{u}_e^*(\tau|t_k)\|_P^2) d\tau \\ &\quad + \|\tilde{p}_e(t_{k+1}+T|t_{k+1})\|_R^2 - \|\tilde{p}_e^*(t_k+T|t_k)\|_R^2 \\ &= -\int_{t_k}^{t_{k+1}} (\|\tilde{p}_e^*(\tau|t_k)\|_Q^2 + \|\tilde{u}_e^*(\tau|t_k)\|_P^2) d\tau \\ &\quad + \int_{t_k+T}^{t_{k+1}+T} (\|\tilde{p}_e(\tau|t_{k+1})\|_Q^2 + \|\tilde{u}_e(\tau|t_{k+1})\|_P^2) d\tau \\ &\quad + \|\tilde{p}_e(t_{k+1}+T|t_{k+1})\|_R^2 - \|\tilde{p}_e^*(t_k+T|t_k)\|_R^2. \end{aligned} \tag{47}$$

By integrating (15) from $t_k + T$ to $t_{k+1} + T$, it follows that

$$\begin{aligned} &\|\tilde{p}_e(t_{k+1}+T|t_{k+1})\|_R^2 - \|p_e^*(t_k+T|t_k)\|_R^2 \\ &+ \int_{t_k+T}^{t_{k+1}+T} L(\tilde{p}_e(\tau), \tilde{u}_e(\tau)) d\tau \le 0. \end{aligned} \tag{48}$$

Substituting (48) into (47), we have $\Delta V \le 0$, which implies that the tracking error for the nominal system converges to the origin asymptotically.

Due to the asymptotic stability of the nominal system, there exists a $\mathcal{KL}$ function $\beta(\cdot,\cdot)$, such that

$$\|\tilde{p}_e^*(t)\| \le \beta(\|\tilde{p}_e^*(t_0)\|, t), \quad \forall t > t_0. \tag{49}$$

Furthermore, because of $p_{fe} \in \mathbb{P}_{fe}$ for all $t > t_0$, there exists a $\mathcal{K}$ function $\gamma(\cdot)$ such that

$$\|p_{fe}(t)\| \le \gamma(\eta), \quad \forall t > t_0. \tag{50}$$

It follows from $p_e(t) = R(\theta_f)(\tilde{p}_e^*(t) + p_{fe}(t))$ and $p_{fe}(0) = 0$ that

$$\|p_e(t)\| \le \beta(\|p_e(t_0)\|, t) + \gamma(\eta). \tag{51}$$

Therefore, the solution of system (9) is asymptotically ultimately bounded with Algorithm 1 and the closed-loop system is ISS. □

4. NRMPC

In this section, an NRMPC strategy is developed. The state of the nominal system is updated by actual state at each sampling instant. Unlike tube-MPC, the control sequence obtained is optimal with respect to the current actual state, and only the first portion of the control is applied to the real system. The optimization problem of the NRMPC strategy is defined as follows:

Problem 2.

$$\min_{\tilde{u}_f(\tau|t_k)} \quad J(\tilde{p}_e(t_k), \tilde{u}_e(t_k)), \tag{52}$$

$$\text{s.t.} \quad \tilde{\xi}_f(t_k|t_k) = \xi_f(t_k), \tag{53}$$

$$\dot{\tilde{\xi}}_f(\tau|t_k) = f_h(\tilde{\xi}_f(\tau|t_k), \tilde{u}_f(\tau|t_k)), \tag{54}$$

$$\tilde{u}_f(\tau|t_k) \in \mathbb{U}, \tag{55}$$

$$\|\tilde{p}_e(\tau|t_k)\| \le \frac{rT}{\tau - t_k}, \tag{56}$$

$$\tilde{p}_e(t_k + T|t_k) \in \Omega_\varepsilon, \tag{57}$$

where $r = \frac{a(1-\lambda_r)}{\sqrt{\bar{k}_1^2+\bar{k}_2^2}}$, $\Omega_\varepsilon = \{\tilde{p}_e : \|\tilde{p}_e\| \le \varepsilon\}$, and $\varepsilon < r$.

Problem 2 yields a minimizing control sequence over the interval $[t_k, t_k + T)$ of the same form as in (25) as well as a minimizing trajectory as in (26). The control input over $[t_k, t_{k+1})$ is chosen as

$$u_f(t) = \tilde{u}_f^*(t|t_k), \quad t \in [t_k, t_{k+1}). \tag{58}$$

The NRMPC strategy is then described in Algorithm 2.

Algorithm 2 NRMPC

1: At time t_k, initialize the nominal system state by the actual one $\tilde{\xi}_f(t_k) = \xi_f(t_k)$.
2: Solve Problem 2 based on the nominal system to obtain the minimizing control sequence $\tilde{\boldsymbol{u}}_f^*(t_k) = \arg\min_{\tilde{u}_f(\tau|t_k)} J(\tilde{p}_e(t_k), \tilde{u}_e(t_k))$.
3: Apply the first portion of the sequence to the real system, i.e., $u_f(t) = \tilde{u}_f^*(t|t_k)$, during the interval $t \in [t_k, t_{k+1})$.
4: Update the time instant $t_k \to t_{k+1}$ and go to step 1.

Remark 7. For Problem 2, the state of nominal system is updated by the actual one at each step. As a result, the optimization problem has to be solved on-line. However, such an updating strategy yields an optimal control with respect to the current state. The scheme has the same computational burden as the deterministic MPC.

Remark 8. Note that the input domain of NRMPC is larger than that of tube-MPC. NRMPC may therefore have better tracking capability.

Remark 9. As shown in Algorithm 2, an open-loop control action is applied to the real system during each sampling interval. However, the existence of disturbances may lead to an error between the actual trajectory and the optimal prediction. This increases the difficulty of analyzing the recursive feasibility using the conventional methods for MPC.

The following two lemmas guarantee recursive feasibility of Problem 2. Lemma 4 states the existence of the control sequence that is able to drive the state of the nominal system into Ω_ε in prediction horizon T, and Lemma 5 shows that the state constraint is satisfied by employing that control sequence to the nominal system.

Lemma 4. *For the tracking control system (9), assume that there exists an optimal control sequence $\tilde{\boldsymbol{u}}_f^*(t_k)$ at instant t_k such that $\tilde{p}_e(t_k+T|t_k) \in \Omega_\varepsilon$, and apply the first control of the sequence to the perturbed system (5). Then, there exists a control sequence $\tilde{\boldsymbol{u}}_f(t_{k+1})$ at t_{k+1} such that $\tilde{p}_e(t_{k+1}+T|t_{k+1}) \in \Omega_\varepsilon$, if*

$$\eta \le \frac{e^{-aT}}{\delta}(r-\varepsilon), \quad \tilde{k}\delta \ge \ln\frac{r}{\varepsilon}, \tag{59}$$

where $\tilde{k} = \min\{\tilde{k}_1, \tilde{k}_2\}$, r and ε are defined in Problem 2.

Proof. Since Problem 2 is feasible at t_k, applying the first portion of the control $\tilde{\boldsymbol{u}}_f^*$ during the interval $[t_k, t_{k+1})$ to the real system may lead to a difference of the trajectory between the actual system and the nominal system. At t_{k+1}, this difference is bounded by

$$\begin{aligned}
&\|\xi_f(t_{k+1}) - \tilde{\xi}_f^*(t_{k+1}|t_k)\| \\
&= \| \xi_f(t_k) + \int_{t_k}^{t_{k+1}} \left[f_h(\xi_f(\tau), \tilde{u}_f^*(\cdot)) + d(\tau) \right] d\tau \\
&\quad - \tilde{\xi}_f^*(t_k|t_k) - \int_{t_k}^{t_{k+1}} f_h(\tilde{\xi}_f^*(\tau|t_k), \tilde{u}_f^*(\cdot)) d\tau \ \| \\
&\le \eta\delta + a\int_{t_k}^{t_{k+1}} \|\xi_f(\tau) - \tilde{\xi}_f^*(\tau|t_k)\| d\tau \\
&\le \eta\delta e^{a\delta}.
\end{aligned} \tag{60}$$

We construct a feasible control sequence at t_{k+1} for the nominal system as follows:

$$\tilde{u}_f(\tau|t_{k+1}) = \begin{cases} \tilde{u}_f^*(\tau|t_k), & \tau \in [t_{k+1}, t_k+T), \\ \tilde{u}_f^\kappa(\tau|t_k), & \tau \in [t_k+T, t_{k+1}+T). \end{cases} \tag{61}$$

First, consider the interval $\tau \in [t_{k+1}, t_k+T)$. Since the state of the nominal system is updated by $\tilde{\xi}(t_{k+1}|t_{k+1}) = \xi(t_{k+1})$, we have

$$\begin{aligned}
&\|\tilde{\xi}_f(\tau|t_{k+1}) - \tilde{\xi}_f^*(\tau|t_k)\| \\
&= \| \xi_f(t_{k+1}) + \int_{t_{k+1}}^{\tau} f_h(\tilde{\xi}_f(s|t_{k+1}), \tilde{u}_f^*(s|t_k)) ds \\
&\quad - \tilde{\xi}_f^*(t_{k+1}|t_k) - \int_{t_{k+1}}^{\tau} f_h(\tilde{\xi}_f^*(s|t_k), \tilde{u}_f^*(s|t_k)) ds \ \| . \\
&\le \eta\delta e^{a\delta} + a\int_{t_{k+1}}^{\tau} \|\tilde{\xi}_f(s|t_{k+1}) - \tilde{\xi}_f^*(s|t_k)\| ds.
\end{aligned} \tag{62}$$

Applying Grönwall–Bellman inequality yields

$$\|\tilde{\xi}_f(\tau|t_{k+1}) - \tilde{\xi}_f^*(\tau|t_k)\| \le \eta\delta e^{a(\tau - t_{k+1} + \delta)}. \tag{63}$$

Substituting t_k+T into (63) leads to

$$\|\tilde{\xi}_f(t_k+T|t_{k+1}) - \tilde{\xi}_f^*(t_k+T|t_k)\| \le \eta\delta e^{aT}. \tag{64}$$

Due to the fact $\|\tilde{p}_e(t_k+T|t_{k+1}) - \tilde{p}_e^*(t_k+T|t_k)\| \le \|\tilde{\xi}_f(t_k+T|t_{k+1}) - \tilde{\xi}_f^*(t_k+T|t_k)\|$ and the application of triangle inequality, we arrive at

$$\|\tilde{p}_e(t_k+T|t_{k+1})\| \le \|\tilde{p}_e^*(t_k+T|t_k)\| + \eta\delta e^{aT}. \tag{65}$$

Since $\tilde{p}_e^*(t_k+T|t_k) \in \Omega_\varepsilon$, i.e. $\|\tilde{p}_e^*(t_k+T|t_k)\| \le \varepsilon$, and $\eta \le \frac{e^{-aT}}{\delta}(r-\varepsilon)$, we obtain

$$\|\tilde{p}_e(t_k+T|t_{k+1})\| \le r, \tag{66}$$

which implies $\tilde{p}_e(t_k+T|t_{k+1}) \in \Omega$.

Next, consider the interval $\tau \in [t_k+T, t_{k+1}+T)$, during which the local controller $\tilde{u}_f^\kappa(\tau|t_k)$ is applied to the nominal system

$$\begin{aligned}
\frac{d}{d\tau}\|\tilde{p}_e(\tau|t_{k+1})\|^2 &= -2(\tilde{k}_1\tilde{x}_e^2 + \tilde{k}_2\tilde{y}_e^2) \\
&\le -2\tilde{k}\|\tilde{p}_e(\tau|t_{k+1})\|^2.
\end{aligned}$$

Applying the comparison principle yields

$$\|\tilde{p}_e(t_{k+1}+T|t_{k+1})\| \le \|\tilde{p}_e(t_k+T|t_{k+1})\| e^{-\delta\tilde{k}}.$$

It follows from $\tilde{k}\delta \ge \ln\frac{r}{\varepsilon}$ that

$$\|\tilde{p}_e(t_{k+1}+T|t_{k+1})\| \le \varepsilon. \tag{67}$$

This proves the existence of a control sequence at t_{k+1} which is able to drive the tracking error of the nominal system into the terminal region Ω_ε. □

Lemma 5. *For the tracking control system (9), assume that there exists an optimal control sequence $\tilde{\boldsymbol{u}}_f^*(t_k)$ at instant t_k such that the trajectory constraint is satisfied, i.e., $\tilde{p}_e^*(\tau|t_k) \le \frac{rT}{\tau - t_k}$, and apply the first control of the sequence to the perturbed system (5). Then, at t_{k+1}, by the control sequence (61), the trajectory constraint is also satisfied if the parameter ε satisfies*

$$\varepsilon \ge \frac{r(T-\delta)}{T}. \tag{68}$$

Proof. To prove $\|\tilde{p}_e(\tau|t_{k+1})\| \le \frac{rT}{\tau - t_{k+1}}$ over the interval $\tau \in [t_{k+1}, t_{k+1}+T)$, we first consider the interval $\tau \in [t_{k+1}, t_k+T)$. From (63), it follows that

$$\|\tilde{p}_e(\tau|t_{k+1})\| \le \|\tilde{p}_e^*(\tau|t_k)\| + \eta\delta e^{aT}. \tag{69}$$

Due to (59) and $\tilde{p}_e^*(\tau|t_k) \le \frac{T}{\tau - t_k}$, we obtain

$$\|\tilde{p}_e(\tau|t_{k+1})\| \le \frac{rT}{\tau - t_k} + (r - \varepsilon). \tag{70}$$

From (68), we have

$$r - \varepsilon \le \frac{\delta r}{T - \delta} \le \frac{\delta r T}{(\tau - t_{k+1})(\tau - t_k)}. \tag{71}$$

Substituting (71) into (70), we obtain

$$\|\tilde{p}_e(\tau|t_{k+1})\| \le \frac{rT}{\tau - t_{k+1}}, \tag{72}$$

which proves that the state constraint is satisfied over the interval $\tau \in [t_{k+1}, t_k+T)$.

Next, consider the interval $\tau \in [t_k+T, t_{k+1}+T)$. By Lemma 4, it holds that $\|\tilde{p}_e(t_k+T|t_{k+1})\| \le r$ once $\|\tilde{p}_e^*(t_k+T|t_k)\| \le \varepsilon$. Since $\frac{rT}{\tau - t_{k+1}} \ge r$, $\|\tilde{p}_e(\tau|t_{k+1})\| \le \frac{rT}{\tau - t_{k+1}}$ is naturally satisfied over the interval $\tau \in [t_k+T, t_{k+1}+T)$, thereby completing the proof. □

Theorem 2. *For the tracking control system (9), suppose that Problem 1 is feasible at time t_0 and the parameters satisfy the conditions in Lemmas 4* and *5. Then,*

(i) *Problem 1 is feasible for all $t_k > t_0$;*
(ii) *the tracking control system (9) is ISS if*

$$\begin{aligned}
\underline{q}\varepsilon^2 &> \frac{1}{2}\eta e^{aT}(r+\varepsilon) + \frac{q^2\eta^2\delta}{2a}(e^{2aT} - e^{2a\delta}) \\
&\quad + \frac{2q^2\eta r}{\sqrt{2a}}\left(\frac{T^2}{\delta} - T\right)^{\frac{1}{2}}(e^{2aT} - e^{2a\delta})^{\frac{1}{2}},
\end{aligned} \tag{73}$$

where $\underline{q} = \min\{q_1, q_2\}$.

Proof. (i) Assume Problem 2 is feasible at instant t_k, then feasibility of Problem 2 at t_{k+1} implies the existence of a control sequence that is able to drive the state of the nominal system to the terminal region Ω_ε while satisfying all the constraints. In terms of Algorithm 2, the first control of the optimal control sequence is applied to the system. From Lemma 4, at t_{k+1}, a feasible control sequence in (61) renders $\tilde{p}_e(t_{k+1}+T|t_{k+1}) \in \Omega_\varepsilon$ while satisfying $\tilde{u}_f(\tau|t_{k+1}) \in \Omega$ for $\tau \in [t_{k+1}, t_{k+1}+T)$. Meanwhile, from Lemma 5, by applying the control sequence (61) to the nominal system (10), the trajectory constraint is satisfied, i.e., $\|\tilde{p}_e(\tau|t_{k+1})\| \le \frac{rT}{\tau - t_{k+1}}$, implying the feasibility of Problem 2 at t_{k+1}. Hence, the feasibility of Problem 2 at the initial time t_0 results in the feasibility for all $t > t_0$ by induction.

(ii) Choose a Lyapunov function as follows

$$V(p_e(t_k)) = J(\tilde{p}_e^*(t_k), \tilde{u}_e^*(t_k)). \tag{74}$$

According to Riemann integral principle, there exists a constant $0 < c_1 \le \delta$ such that

$$V(p_e) \ge c_1 L(p_e, u_e) \triangleq \alpha_1(\|p_e\|), \tag{75}$$

where $\alpha_1(\cdot)$ is obviously a $\mathcal{K}_\infty$ function. On the other hand, from (15), we have

$$V(p_e(t_k)) \le g(p_e(t_k)) + g(p_e(t_k+T|t_k)), \forall p_e \in \Omega_\varepsilon.$$

Due to the decreasing property of $g(\cdot)$ in Ω_ε with respect to time, it follows that

$$V(p_e(t_k)) \le 2g(p_e(t_k)), \quad \forall p_e \in \Omega_\varepsilon. \tag{76}$$

Because the origin lies in the interior of Ω_ε and $2g(p_e(t)) \le \varepsilon$, $\forall p_e \in \Omega_\varepsilon$, it holds that $2g(p_e(t)) \ge \varepsilon$ if $p_e \in \mathbb{R}^{2\times 2} \setminus \Omega_\varepsilon$. Due to the feasibility of Problem 2, there exists an upper-bound $c_2 > \varepsilon$ for $V(p_e(t))$. Thus $\alpha_2(\|p_e\|) = \frac{c_2}{\varepsilon} g(p_e(t))$ is a $\mathcal{K}_\infty$ function such that $\alpha_2(\|p_e\|) \ge c_2$ thereby satisfying $\alpha_2(\|p_e(t)\|) \ge V(p_e(t))$. This proves the existence of $\mathcal{K}_\infty$ functions $\alpha_1(\cdot)$ and $\alpha_2(\cdot)$ satisfying

$$\alpha_1(\|p_e(t)\|) \le V(p_e(t)) \le \alpha_2(\|p_e(t)\|). \tag{77}$$

The difference of the Lyapunov function at t_k and t_{k+1} satisfies

$$\begin{aligned} \Delta V &= V(p_e(t_{k+1})) - V(p_e(t_k)) \\ &\le J(\tilde{p}_e(t_{k+1}), \tilde{u}_e(t_{k+1})) - J(\tilde{p}_e^*(t_k), \tilde{u}_e^*(t_k)) \\ &\triangleq \Delta V_1 + \Delta V_2 + \Delta V_3, \end{aligned} \tag{78}$$

in which

$$\begin{aligned} \Delta V_1 &= \int_{t_{k+1}}^{t_k+T} (\|\tilde{p}_e(\tau|t_{k+1})\|_Q^2 - \|\tilde{p}_e^*(\tau|t_k)\|_Q^2) d\tau, \\ \Delta V_2 &= \int_{t_k+T}^{t_{k+1}+T} (\|\tilde{p}_e(\tau|t_{k+1})\|_Q^2 + \|\tilde{u}_e(\tau|t_{k+1})\|_P^2) d\tau \\ &\quad + \|\tilde{p}_e(t_{k+1}+T|t_{k+1})\|_R^2 - \|\tilde{p}_e^*(t_k+T|t_k)\|_R^2, \\ \Delta V_3 &= -\int_{t_k}^{t_{k+1}} (\|\tilde{p}_e^*(\tau|t_k)\|_Q^2 + \|\tilde{u}_e^*(\tau|t_k)\|_P^2) d\tau. \end{aligned}$$

For ΔV_1, it holds that

$$\begin{aligned} \Delta V_1 \le & \int_{t_{k+1}}^{t_k+T} (\|\tilde{p}_e(\tau|t_{k+1}) - \tilde{p}_e^*(\tau|t_k)\|_Q) \\ & \times (\|\tilde{p}_e(\tau|t_{k+1})\|_Q + \|\tilde{p}_e^*(\tau|t_k)\|_Q) d\tau. \end{aligned} \tag{79}$$

By (63), we have

$$\begin{aligned} \Delta V_1 &\le \int_{t_{k+1}}^{t_k+T} [q^2\eta\delta e^{a(\tau+\delta-t_{k+1})}(2\|\tilde{p}_e^*(\tau|t_k)\| \\ &\quad + \eta\delta e^{a(\tau+\delta-t_{k+1})})] d\tau \\ &= \int_{t_{k+1}}^{t_k+T} [2q^2\eta\delta e^{a(\tau+\delta-t_{k+1})}\|\tilde{p}_e^*(\tau|t_k)\| \\ &\quad + q^2\eta^2\delta^2 e^{2a(\tau+\delta-t_{k+1})}] d\tau \\ &\le \int_{t_{k+1}}^{t_k+T} 2q^2\eta\delta e^{a(\tau+\delta-t_{k+1})}\|\tilde{p}_e^*(\tau|t_k)\| d\tau \\ &\quad + \frac{q^2\eta^2\delta^2}{2a}(e^{2aT} - e^{2a\delta}). \end{aligned} \tag{80}$$

Applying Hölder inequality to the first term of the last inequality yields

$$\begin{aligned} \Delta V_1 &\le \left(\int_{t_{k+1}}^{t_k+T} \|\tilde{p}_e^*(\tau|t_k)\|^2 d\tau\right)^{\frac{1}{2}} \frac{2q^2\eta\delta}{\sqrt{2a}}(e^{2aT} - e^{2a\delta})^{\frac{1}{2}} \\ &\quad + \frac{q^2\eta^2\delta^2}{2a}(e^{2aT} - e^{2a\delta}) \\ &\le \frac{2q^2\eta\delta r}{\sqrt{2a}}(\frac{T^2}{\delta} - T)^{\frac{1}{2}}(e^{2aT} - e^{2a\delta})^{\frac{1}{2}} \\ &\quad + \frac{q^2\eta^2\delta^2}{2a}(e^{2aT} - e^{2a\delta}). \end{aligned} \tag{81}$$

Rewrite ΔV_2 as

$$\begin{aligned} \Delta V_2 &= \int_{t_k+T}^{t_{k+1}+T} (\|\tilde{p}_e(\tau|t_{k+1})\|_Q^2 + \|\tilde{u}_e(\tau|t_{k+1})\|_P^2 d)\tau \\ &\quad + \|\tilde{p}_e(t_{k+1}+T|t_{k+1})\|_R^2 - \|\tilde{p}_e^*(t_k+T|t_k)\|_R^2 \\ &\quad + \|\tilde{p}_e(t_k+T|t_{k+1})\|_R^2 - \|\tilde{p}_e(t_k+T|t_{k+1})\|_R^2. \end{aligned} \tag{82}$$

Integrating (15) from t_k+T to $t_{k+1}+T$ and substituting it into (82) leads to

$$\begin{aligned} \Delta V_2 &\le \|\tilde{p}_e(t_k+T|t_{k+1})\|_R^2 - \|\tilde{p}_e^*(t_k+T|t_k)\|_R^2 \\ &\le (\frac{1}{2}\|\tilde{p}_e(t_k+T|t_{k+1}) - \tilde{p}_e^*(t_k+T|t_k)\|) \\ &\quad \times \left(\|\tilde{p}_e(t_k+T|t_{k+1})\| + \|\tilde{p}_e^*(t_k+T|t_k)\|\right) \\ &\le \frac{1}{2}\eta\sigma e^{aT}(\varepsilon + r). \end{aligned} \tag{83}$$

For ΔV_3, we first assume $\|\tilde{p}_e(t_{k+1}|t_k)\| > \varepsilon$, which implies $\|\tilde{p}_e(\tau|t_k)\| > \varepsilon$, $\tau \in [t_k, t_{k+1})$, and thus we obtain

$$\Delta V_3 < -\int_{t_k}^{t_{k+1}} \|\tilde{p}_e^*(\tau|t_k)\|_Q^2 d\tau \le -\underline{q}\delta\varepsilon^2. \tag{84}$$

In combination with (81), (83) and (84), the inequality (78) thus satisfies

$$\begin{aligned} \Delta V &< -\underline{q}\delta\varepsilon^2 + \frac{1}{2}\eta\delta e^{aT}(r+\varepsilon) + \frac{q^2\eta^2\delta^2}{2a}(e^{2aT} - e^{2a\delta}) \\ &\quad + \frac{2q^2\eta\delta r}{\sqrt{2a}}(\frac{T^2}{\delta} - T)^{\frac{1}{2}}(e^{2aT} - e^{2a\delta})^{\frac{1}{2}}. \end{aligned} \tag{85}$$

From (73), $\Delta V < 0$ holds. It follows from Theorem 2 of Michalska and Mayne (1993) that $\|\tilde{p}_e^*(t_k|t_k)\| \le \varepsilon$ for $t_k \ge t_f$, where $t_f > t_0$ is a finite time instant. When the tracking error enters into the terminal region, i.e., $p_e(t_k) \in \Omega_\varepsilon$, reconsider ΔV_1 and ΔV_3:

$$\begin{aligned} \Delta V_1 &\le \int_{t_{k+1}}^{t_k+T} 2q^2\eta\delta\varepsilon e^{a(\tau-t_{k+2})} d\tau + \frac{q^2\eta^2\delta^2}{2a}(e^{2aT} - e^{2a\delta}) \\ &= \frac{2q^2\eta\delta\varepsilon}{a}(e^{aT} - e^{a\delta}) + \frac{q^2\eta^2\delta^2}{2a}(e^{2aT} - e^{2a\delta}). \end{aligned}$$

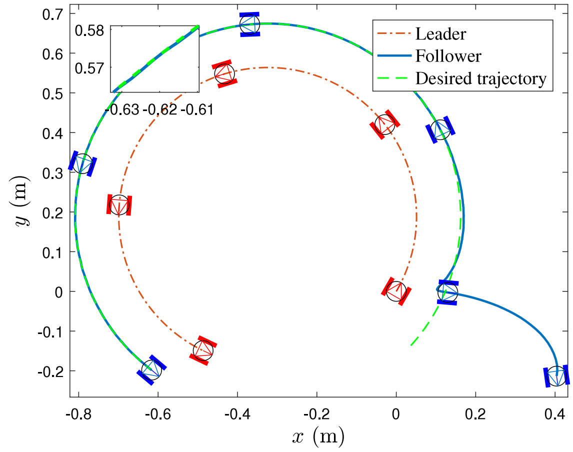

Fig. 3. Tracking trajectories by using tube-MPC.

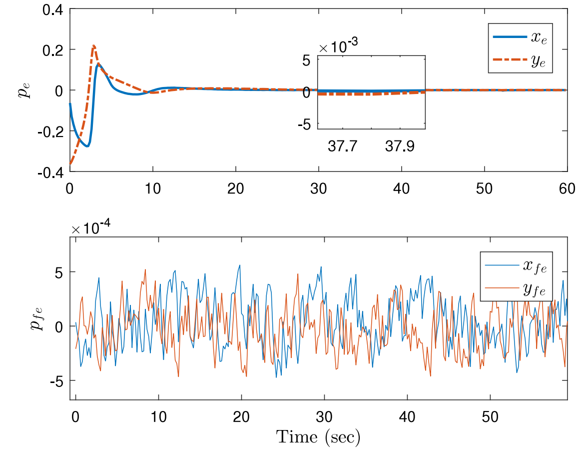

Fig. 4. Tracking errors by using tube-MPC.

Due to the decreasing property of $\|\tilde{p}_e^*(\tau|t_k)\|_Q^2$ in Ω_ε, it follows that

$$\Delta V_3 \leq -\underline{q}\delta\|p_e^*(t_{k+1}|t_k)\|^2.$$

Since $\|\tilde{p}_e^*(\tau|t_{k+1})\| \leq \|\tilde{p}_e^*(\tau|t_k)\| + \eta\delta e^{aT}$, we have $\|p_e(t_{k+1})\|^2 \leq \|p_e^*(t_{k+1}|t_k)\|^2 + \eta^2\delta^2 e^{2a\delta} + 2\varepsilon\eta\delta e^{a\delta}$. Consequently,

$$\Delta V_3 \leq -\underline{q}\delta\|p_e(t_{k+1})\|^2 + \underline{q}\eta^2\delta^3 e^{2a\delta} + 2\underline{q}\varepsilon\eta\delta^2 e^{a\delta}.$$

As a result, it holds that

$$\Delta V \leq -\underline{q}\delta\|p_e(t_{k+1})\|^2 + \sigma(\eta), \tag{86}$$

where $\sigma(\eta) = \frac{2q^2\eta\delta\varepsilon}{a}(e^{aT} - e^{a\delta}) + \frac{q^2\eta^2\delta^2}{2a}(e^{2aT} - e^{2a\delta}) + \frac{1}{2}\eta\sigma e^{aT}(\varepsilon + r) + \underline{q}\eta^2\delta^3 e^{2a\delta} + 2\underline{q}\varepsilon\eta\delta^2 e^{a\delta}$ is obviously a $\mathcal{K}$ function with respect to η. Hence, the theorem is proved. □

5. Simulation results

The simulation is implemented on a PC equipped with a dual-core 3.20 GHz Intel i5 CPU, 7.88 GB RAM and 64-bit Windows 10 operating system. The optimization problem is transcribed by Tool Box ICLOCS (Imperial College London Optimal Control Software, see Falugi, Kerrigan, & Wyk, 0000), 1.2 version, and solved by NLP (Nonlinear Programming) solver IPOPT (Interior Point OPTimizer, see Wächter & Biegler, 2006), 3.11.8 version.

The mechanism parameters of the two homogeneous robots used in the simulation are taken from an educational robot named E-puck (Mondada et al., 2009), and are given by $a = 0.13$ m/s, $\rho = 0.0267$ m and $b = a/\rho = 4.8598$ rad/s. The trajectory to be tracked is a circular motion with linear velocity $v_r = 0.015$ m/s, angular velocity $\omega_r = 0.04$ rad/s and initial configuration $\xi_r(t_0) = [0, 0, \frac{\pi}{3}]^{\mathrm{T}}$. The initial configuration of the follower is set to be $\xi_f(t_0) = [0.2, -0.2, -\frac{\pi}{2}]^{\mathrm{T}}$ and its desired separation with respect to the frame fixed on the leader is set to be $p_d = [-0.1, -0.1]^{\mathrm{T}}$. The disturbances are bounded by $\eta = 0.004$. For the tracking objective, the prediction horizon and the sampling period are set to be $T = 2$ s and $\delta = 0.2$ s, respectively. The positive definite matrices P and Q are chosen, according to Lemma 1, as $P = \text{diag}\{0.4, 0.4\}$ and $Q = \text{diag}\{0.2, 0.2\}$, respectively. The feedback gains for the terminal controller are set to be $\tilde{k}_1 = \tilde{k}_2 = 1.2$ to satisfy the requirements given by Lemma 1. First, let us design tube-MPC according to Lemma 3 and Theorem 1. We set the feedback gain to be $K = \text{diag}\{-2.3, -2.3\}$. The control input constraint for Problem 1 is $\mathbb{U}_{\text{tube}} = \lambda_{\text{tube}}\mathbb{U}$ with $\lambda_{\text{tube}} = 0.6636$, and the terminal region is given by $\Omega_{\text{tube}} = \{\tilde{p}_e : |\tilde{x}_e| + |\tilde{y}_e| \leq 0.0542\}$. Applying Algorithm 1 to the tracking system yields the tracking trajectory as shown in Fig. 3. To evaluate the tracking performance, we take the tracking error p_e and the real position deviation from the center of the tube p_{fe} as indexes. As shown in Fig. 4, the tracking error converges to a neighborhood of the origin. Fig. 5 indicates that the trajectory of the follower lies in tube $\mathbb{T} = \tilde{p}_f^* \oplus \mathbb{P}_{fe}$ with $\mathbb{P}_{fe} = \{|p_{fe}| \leq [0.0017, 0.0017]^{\mathrm{T}}\}$, which is obtained from Lemma 3. Fig. 6 shows the control input performance of the follower. We also take $|v|/a + |\omega|/b$ as an index to evaluate the input constraint. The fluctuated control signal indicates the effectiveness of the feedback part of the controller which reduces the tracking error caused by the disturbances. Furthermore, the input constraint $\mathbb{U}_{\text{tube}}$ for the nominal system is active over the interval $t \in [0, 3]$, while the constraint $\mathbb{U}$ for the real system is not active, which indicates the weak control ability.

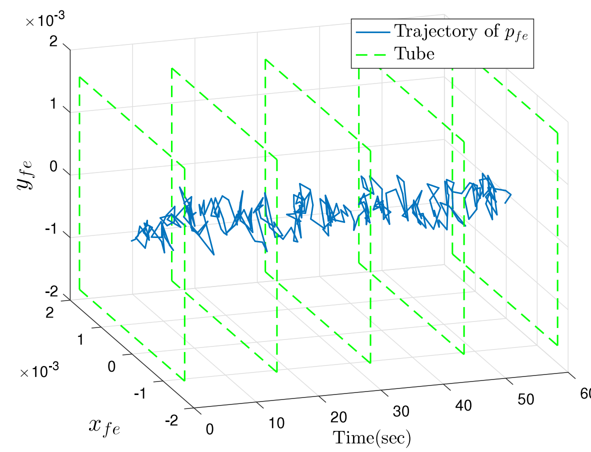

Fig. 5. The error between actual and nominal states lies in a tube.

To show the effect of different choices of the feedback gain K on the tracking performance, we set $K = \text{diag}\{-1, -1\}$ and $K = \text{diag}\{-4, -4\}$, respectively, to observe the difference between the actual trajectory and the optimal one. As shown in Fig. 7, increasing of K reduces the difference of the actual position and the center of the tube and therefore improves the tracking performance.

Next, design NRMPC according to Lemmas 4, 5 and Theorem 2. The input constraint of NRMPC differs from the constraint of tube-MPC and is given by $\tilde{u}_f \in \mathbb{U}$ according to Algorithm 2. The terminal region is designed as $\Omega_\varepsilon = \{\tilde{p}_e : \|\tilde{p}_e\| \leq 0.063\}$, and consequently $\varepsilon = 0.063$, which satisfies the conditions in Lemmas 4, 5 and Theorem 2. Fig. 8 shows the tracking trajectory and Fig. 9 presents the

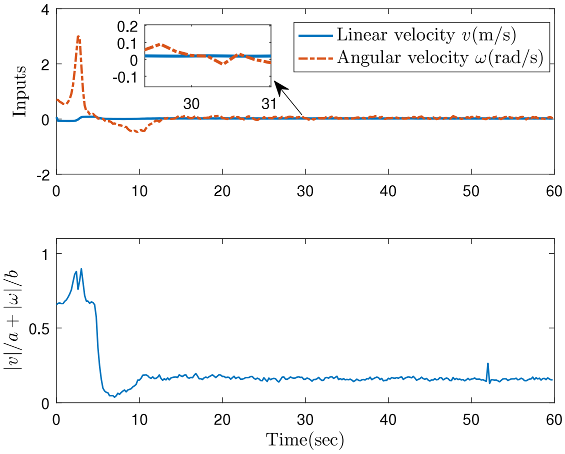

Fig. 6. Control input of tube-MPC.

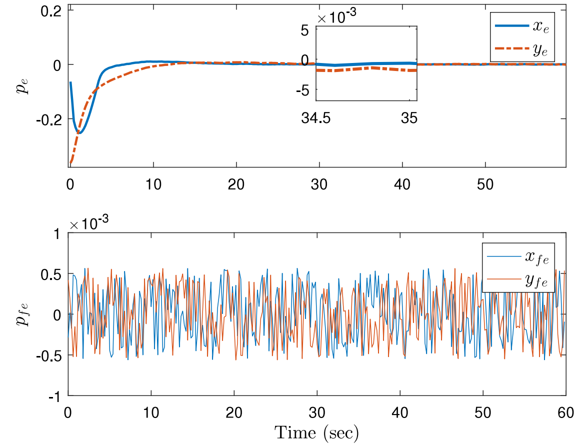

Fig. 9. Tracking errors by using NRMPC.

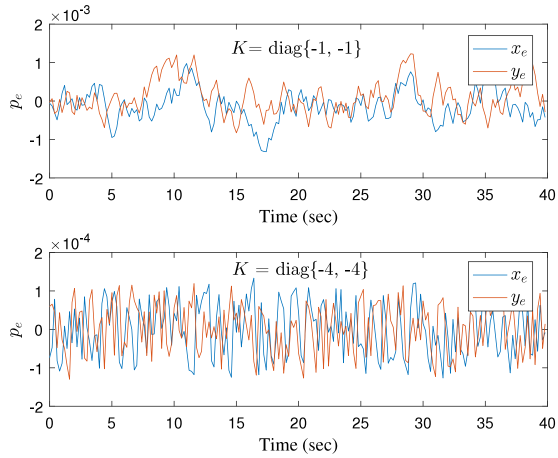

Fig. 7. Real-time position deviation from the center of the tube p_{fe} with different feedback gains.

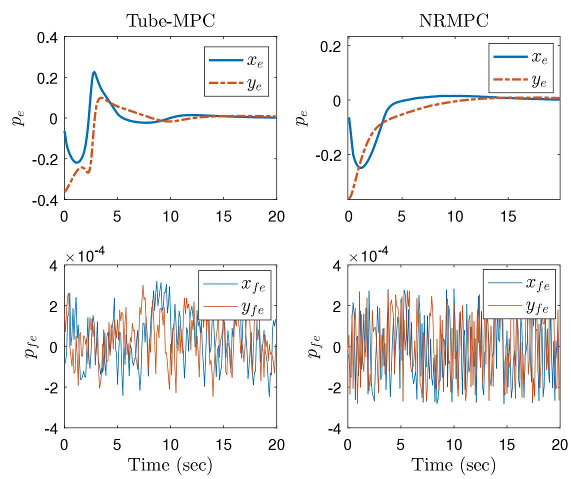

Fig. 10. Tracking errors of tube-MPC and NRMPC with $\delta = 0.1$ s.

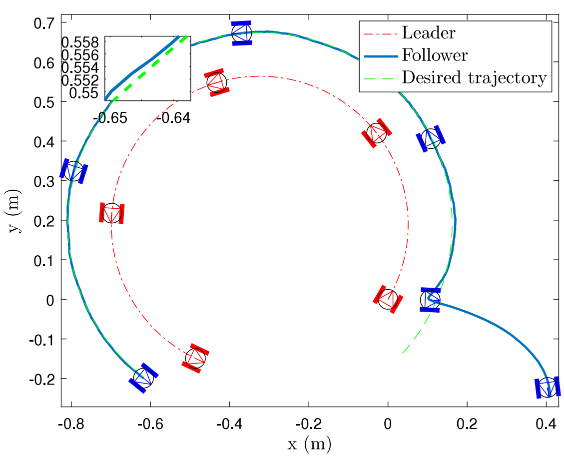

Fig. 8. Tracking trajectories by using NRMPC.

tracking errors by Algorithm 2. It can be observed that the tracking error converges to a neighborhood of the origin. To compare the influence level by disturbances of the two strategies proposed, we define $p_{fe}(t_k) = p_f(t_k) - \tilde{p}_f^*(t_k)$ in NRMPC. It can be seen that the tracking performance is directly influenced by disturbances due to the open-loop control during each sampling period. This indicates that NRMPC has worse steady state performance than tube-MPC, since the latter can work locally for its feedback. To further verify this conclusion, we shorten the sampling time as $\delta = 0.1$ s. As shown in Fig. 10, the shorter sampling interval can enhance the steady state performance of NRMPC but the performance is still not better than tube-MPC for the same sampling period. Fig. 11 shows the control input under NRMPC. According to Algorithm 2, the control signal at each time instant is optimal corresponding to its current state, which indicates its robustness. We also note that the input constraint is active over the interval $t \in [0, 3]$, which demonstrates a better tracking capability.

To further compare tube-MPC with NRMPC, we take cost function J, real stage cost $\|p_e\|_Q^2 + \|u_e\|_P^2$, real state cost $\|p_e\|_Q^2$ and real input cost $\|u_e\|_P^2$ to evaluate the converging performance. Their cost curves are plotted in Fig. 12. As it can be seen, the total cost, the stage cost and the state cost decrease faster by implementing NRMPC than by tube-MPC. However, the input cost of NRMPC is higher than that of tube-MPC. This is explained by the fact that the input constraint of tube-MPC is tighter than that of NRMPC, which may degrade the control capability. This also helps explaining why the tracking error decreases faster by NRMPC than tube-MPC. Fig. 13 provides distribution of the computation time in solving the optimization problems. It shows that there is no significant difference between NRMPC and tube-MPC, which implies that they have almost the same computational complexity.

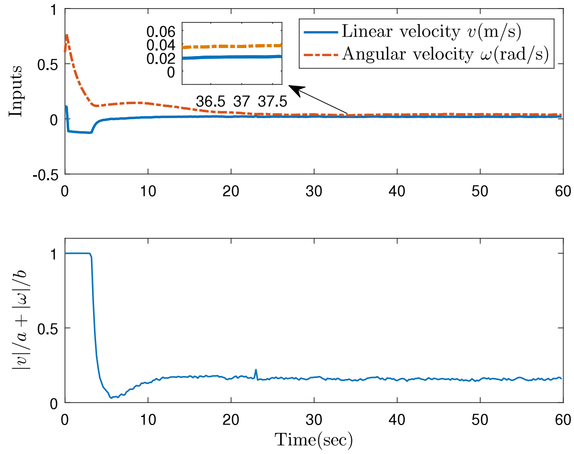

Fig. 11. Control input of NRMPC.

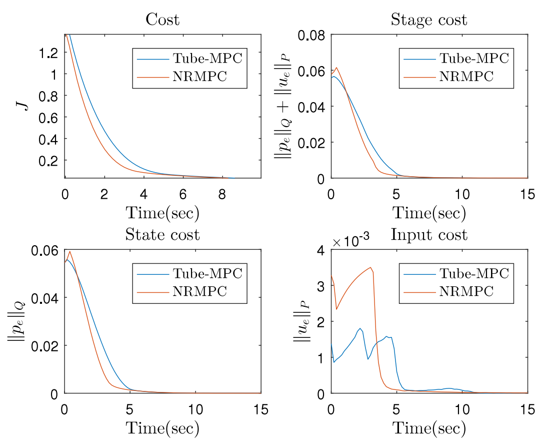

Fig. 12. Costs of tube-MPC and NRMPC.

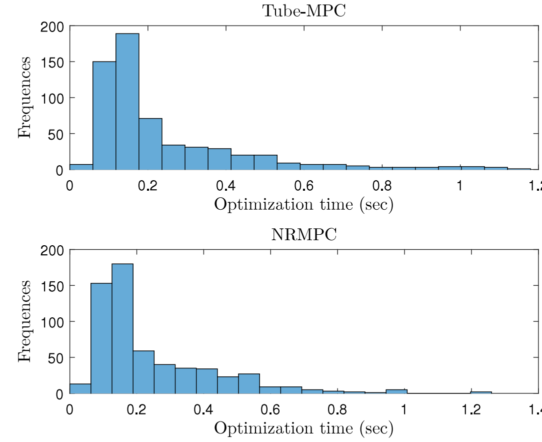

Fig. 13. Distribution of computation time by tube-MPC and NRMPC.

However, as stated in Remark 5, the optimization problem can be solved off-line in tube-MPC, whereas the optimization problem has to be solved on-line in NRMPC.

Remark 10. The optimization time in Fig. 13 is used to compare the computational complexity of the schemes. Optimization time is an important factor that should be considered for application, and many approaches are proposed to reduce it. For example, in Carvalho, Gao, Gray, Tseng, and Borrelli (2013), a customized sequential quadratic programming algorithm is proposed using iterative Jacobian linearization approach to transform nonlinear programming into a quadratic programming. Feedback linearization is used in Farina, Perizzato, and Scattolini (2015) to reduce the computational burden. In Carrau, Liniger, Zhang, and Lygeros (2016) and Zhang et al. (2015), approximating the stochastic MPC problem by means of randomization is applied to reduce the computational complexity. Event- and self-triggered MPC are studied in Eqtami, Heshmati-Alamdari, Dimarogonas, and Kyriakopoulos (2013) and Li and Shi (2014a), which aim at reducing the frequency of solving the optimization problem. Cloud control is proposed in Adaldo, Liuzza, Dimarogonas, and Johansson (2016) and Xia (2015), which share the computation load by virtue of powerful computing capacity of the cloud to simplify the local control device.

Finally, we summarize the simulation study as follows:

(i) Tube-MPC has a better steady state performance than NRMPC. This is because the control strategy of tube-MPC consists of two parts: optimal control and feedback part, while NRMPC is open-loop control during each sampling period. The steady state performance of NRMPC can be improved by shortening sampling period.
(ii) NRMPC performs better in terms of dynamic property than tube-MPC due to the tighter input constraint of tube-MPC.
(iii) The computational complexities of tube-MPC and NRMPC are almost the same. However, the optimization problem in tube-MPC can be solved in a parallel way if the nominal system update manner is taken as formulated in Remark 5, which may enhance its real-time performance.

6. Conclusion

In this paper, two robust MPC strategies have been developed for tracking of unicycle robots with coupled input constraint and bounded disturbances. We first developed a tube-MPC strategy, where the trajectory of the real system is constrained in a tube centered along the optimal nominal trajectory by a nonlinear feedback law based on the deviation of the actual states from the optimal states. Tube-MPC possesses robustness but sacrifices optimality, thus we further developed the NRMPC scheme, where the state of the nominal system is updated by the actual state at each step. It was shown that the tracking control system is ISS under both of the robust MPC strategies, and their optimization problems are feasible. Simulation results illustrated the effectiveness of the two schemes and their respective advantages.

Appendix

Proof of Lemma 1. First, consider the terminal controller

$$
\begin{aligned}
\frac{|\tilde{v}_f^{\kappa}|}{a}+\frac{|\tilde{\omega}_f^{\kappa}|}{b} &= \frac{|\tilde{k}_1\tilde{x}_e+v_f^d|}{a}+\frac{|\tilde{k}_2\tilde{y}_e+\omega_f^d|}{a}\\
&\le \frac{1}{a}(\tilde{k}_1|\tilde{x}_e|+\tilde{k}_2|\tilde{y}_e|+|v_f^d|+|\omega_f^d|)\\
&\le \lambda_f-\lambda_r+\frac{\sqrt{2}}{a}\|D\|\|u_r\|\le\lambda_f,
\end{aligned}
$$

where $v_f^d=(v_r-x_d\omega_r)\cos\tilde{\theta}_e-x_d\omega_r\sin\tilde{\theta}_e$ and $\omega_f^d=\frac{1}{\rho}((v_r-x_d\omega_r)\sin\tilde{\theta}_e+y_d\omega_r\cos\tilde{\theta}_e)$. This implies $u_f^{\kappa}\in\lambda_f\mathbb{U}$ if $\tilde{p}_e\in\Omega$.

Next, choose $g(\tilde{p}_e(\tau|t_k))$ as Lyapunov function. The derivative of $g(\tilde{p}_e(\tau|t_k))$ with respect to τ yields

$$\dot{g}(\tilde{p}_e(\tau|t_k))=-(\tilde{k}_1\tilde{x}_e^2(\tau|t_k)+\tilde{k}_2\tilde{y}_e^2(\tau|t_k)),$$

which means that Ω is invariant by implementing the terminal controller, i.e., $\tilde{p}_e(\tau|t_k) \in \Omega$ holds for all $\tau > t_k$ once $\tilde{p}_e(t_k|t_k) \in \Omega$.

Finally, for $\tilde{p}_e(\tau|t_k) \in \Omega$, it follows that

$$\begin{aligned}
&\dot{g}(\tilde{p}_e(\tau|t_k)) + L(\tilde{p}_e(\tau|t_k), \tilde{u}_e(\tau|t_k)) \\
&= \tilde{x}_f^e \dot{\tilde{x}}_e + \tilde{y}_e \dot{\tilde{y}}_e + q_1 \tilde{x}_e^2 + q_2 \tilde{y}_e^2 + p_1 \tilde{v}_e^2 + p_2 \tilde{\omega}_e^2 \\
&= -\tilde{k}_1 \tilde{x}_e^2 - \tilde{k}_2 \tilde{y}_e^2 + q_1 \tilde{x}_e^2 + q_2 \tilde{y}_e^2 + p_1 \tilde{v}_e^2 + p_2 \tilde{\omega}_e^2 \\
&= (p_1 \tilde{k}_1^2 - \tilde{k}_1 + q_1)\tilde{x}_e^2 + (p_2 \tilde{k}_2^2 - \tilde{k}_2 + q_2)\tilde{y}_e^2.
\end{aligned}$$

Since $p_i q_i < \frac{1}{4}$ and $\tilde{k}_i \in \left(\frac{1-\sqrt{1-4p_iq_i}}{2p_i}, \frac{1+\sqrt{1-4p_iq_i}}{2p_i}\right), i = 1, 2$, the inequality $\dot{g} + L < 0$ holds.

Hence, from Definition 1, Ω is a terminal region associated with the terminal controller $\tilde{u}_f^{\kappa}(\tau|t_k)$. $\square$

Proof of Lemma 2. Considering the function values of $f_h(\xi, u)$ at ξ_1 and ξ_2 with the same u, we have

$$\begin{aligned}
&\|f_h(\xi_1, u) - f_h(\xi_2, u)\|^2 \\
&= \left\| \begin{bmatrix} v(\cos\theta_1 - \cos\theta_2) + \rho\omega(\sin\theta_2 - \sin\theta_1) \\ v(\sin\theta_1 - \sin\theta_2) + \rho\omega(\cos\theta_1 - \cos\theta_2) \\ 0 \end{bmatrix} \right\|^2 \\
&= v^2(\cos\theta_1 - \cos\theta_2)^2 + \rho^2\omega^2(\sin\theta_2 - \sin\theta_1)^2 \\
&\quad + v^2(\sin\theta_1 - \sin\theta_2)^2 + \rho^2\omega^2(\cos\theta_2 - \cos\theta_1)^2 \\
&\le 2(v^2 + \rho^2\omega^2)(\theta_1 - \theta_2)^2 \\
&\le 2 \max_{[v,\omega]^{\mathrm{T}} \in \mathbb{U}} \{v^2 + \rho^2\omega^2\}(\theta_1 - \theta_2)^2 \\
&= a^2(\theta_1 - \theta_2)^2,
\end{aligned}$$

where the mean value theorem and Lagrange multiplier method are used in the last inequality. The maximum of $v^2 + \rho^2\omega^2$, subject to $|v|/a + |\omega|/b \le 1$, can be obtained by setting $v = \frac{a}{2}$ and $\omega = \frac{b}{2}$. From the results above, we conclude that

$$\|f_h(\xi_1, u) - f_h(\xi_2, u)\| \le a\|\xi_1 - \xi_2\|. \quad \square$$

References

Adaldo, A., Liuzza, D., Dimarogonas, D. V., & Johansson, K. H. (2016). Multi-agent trajectory tracking with self-triggered cloud access. In *Proceedings of conference on decision and control* (pp. 2207–2214).

Carrau, J. V., Liniger, A., Zhang, X., & Lygeros, J. (2016). Efficient implementation of Randomized MPC for miniature race cars. In *Proceedings of European control conference* (pp. 957–962).

Carvalho, A., Gao, Y., Gray, A., Tseng, H. E., & Borrelli, F. (2013). Predictive control of an autonomous ground vehicle using an iterative linearization approach. In *Proceedings of International IEEE conference on intelligent transportation systems* (pp. 2335–2340).

Chen, J., Sun, D., Yang, J., & Chen, H. (2010). Leader-follower formation control of multiple nonholonomic mobile robots incorporating receding-horizon scheme. *International Journal of Robotics Research*, *29*, 727–747.

Chisci, L., Rossiter, J. A., & Zappa, G. (2001). Systems with persistent disturbances: predictive control with restricted constraints. *Automatica*, *37*(7), 1019–1028.

Coleman, T. F., & Li, Y. (1996). An interior trust region approach for nonlinear minimization subject to bounds. *SIAM Journal on Optimization*, *6*(2), 418–445.

Dai, L., Xia, Y., Gao, Y., Kouvaritakis, B., & Cannon, M. (2015). Cooperative distributed stochastic MPC for systems with state estimation and coupled probabilistic constraints. *Automatica*, *61*, 89–96.

Das, A. K., Fierro, R., Kumar, V., Ostrowski, J. P., Spletzer, J., & Taylor, Ca. J. (2002). A vision-based formation control framework. *IEEE Transactions on Robotics and Automation*, *18*(5), 813–825.

Desai, J. P., Ostrowski, J. P., & Kumar, V. (2001). Modeling and control of formations of nonholonomic mobile robots. *IEEE Transactions on Robotics and Automation*, *17*(6), 905–908.

Eqtami, A., Heshmati-Alamdari, S., Dimarogonas, D. V., & Kyriakopoulos, K. J. (2013). A self-triggered model predictive control framework for the cooperation of distributed nonholonomic agents. In *Proceedings of conference on decision and control* (pp. 7384–7389).

Falugi, P., Kerrigan, E., & Wyk, E. v. Imperial college london optimal control software. http://www.ee.ic.ac.uk/ICLOCS/.

Farina, M., Perizzato, A., & Scattolini, R. (2015). Application of distributed predictive control to motion and coordination problems for unicycle autonomous robots. *Robotics and Autonomous Systems*, *72*, 248–260.

Fleming, J., Kouvaritakis, B., & Cannon, M. (2015). Robust tube MPC for linear systems with multiplicative uncertainty. *IEEE Transactions on Automatic Control*, *60*(4), 1087–1092.

Frasch, J. V., Gray, A., Zanon, M., Ferreau, H. J., Sager, S., & Borrelli, F. et al. (2013). An auto-generated nonlinear mpc algorithm for real-time obstacle avoidance of ground vehicles. In *Proceedings of European control conference* (pp. 4136–4141).

Gao, Y., Gray, A., Carvalho, A., Tseng, H. E., & Borrelli, F. (2014). Robust nonlinear predictive control for semiautonomous ground vehicles. In *Proceedings of American control conference* (pp. 4913–4918).

Gao, Y., Gray, A., Tseng, H. E., & Borrelli, F. (2014). A tube-based robust nonlinear predictive control approach to semiautonomous ground vehicles. *Vehicle System Dynamics*, *52*(6), 802–823.

Ghommam, J., Mehrjerdi, H., Saad, M., & Mnif, F. (2010). Formation path following control of unicycle-type mobile robots. *Robotics and Autonomous Systems*, *58*(5), 727–736.

Grammatico, S., Subbaraman, A., & Teel, A. R. (2013). Discrete-time stochastic control systems: A continuous Lyapunov function implies robustness to strictly causal perturbations. *Automatica*, *49*(10), 2939–2952.

Gu, D., & Hu, H. (2006). Receding horizon tracking control of wheeled mobile robots. *IEEE Transactions on Control Systems Technology*, *14*(4), 743–749.

Hokayem, P., Cinquemani, E., Chatterjee, D., Ramponi, F., & Lygeros, J. (2012). Stochastic receding horizon control with output feedback and bounded controls. *Automatica*, *48*(1), 77–88.

Jiang, Z. P., & Nijmeijer, H. (1997). Tracking control of mobile robots: a case study in backstepping. *Automatica*, *33*(7), 1393–1399.

Kothare, M. V., Balakrishnan, V., & Morari, M. (1996). Robust constrained model predictive control using linear matrix inequalities. *Automatica*, *32*(10), 1361–1379.

Lafferriere, G., Williams, A., Caughman, J., & Veerman, J. (2005). Decentralized control of vehicle formations. *Systems & Control Letters*, *54*(9), 899–910.

Langson, W., Chryssochoos, I., Raković, S. V., & Mayne, D. Q. (2004). Robust model predictive control using tubes. *Automatica*, *40*(1), 125–133.

Lee, T., Song, K., Lee, C., & Teng, C. (2001). Tracking control of unicycle-modeled mobile robots using a saturation feedback controller. *IEEE Transactions on Control Systems Technology*, *9*(2), 305–318.

Lee, J. H., & Yu, Z. (1997). Worst-case formulations of model predictive control for systems with bounded parameters. *Automatica*, *33*(5), 763–781.

Li, H., & Shi, Y. (2014a). Event-triggered robust model predictive control of continuous-time nonlinear systems. *Automatica*, *50*(5), 1507–1513.

Li, H., & Shi, Y. (2014b). Robust distributed model predictive control of constrained continuous-time nonlinear systems: a robustness constraint approach. *IEEE Transactions on Automatic Control*, *59*(6), 1673–1678.

Limon Marruedo, D., Alamo, T., & Camacho, E. F. (2002a). Input-to-state stable MPC for constrained discrete-time nonlinear systems with bounded additive uncertainties. In *Proceedings of conference on decision and control* (pp. 4619–4624).

Limon Marruedo, D., Alamo, T., & Camacho, E. F. (2002b). Stability analysis of systems with bounded additive uncertainties based on invariant sets: Stability and feasibility of MPC. In *Proceedings of American control conference* (pp. 364–369).

Limón, D., Alamo, T., Salas, F., & Camacho, E. F. (2006). Input to state stability of min–max MPC controllers for nonlinear systems with bounded uncertainties. *Automatica*, *42*(5), 797–803.

Marshall, J. A., Broucke, M. E., & Francis, B. A. (2006). Pursuit formations of unicycles. *Automatica*, *42*(1), 3–12.

Mayne, D. (2016). Robust and stochastic model predictive control: Are we going in the right direction? *Annual Reviews in Control*, *41*, 184–192.

Mayne, D. Q., Kerrigan, E. C., Van Wyk, E. J., & Falugi, P. (2011). Tube-based robust nonlinear model predictive control. *International Journal of Robust and Nonlinear Control*, *21*(11), 1341–1353.

Mayne, D. Q., & Langson, W. (2001). Robustifying model predictive control of constrained linear systems. *Electronics Letters*, *37*(23), 1422–1423.

Mayne, D. Q., Rawlings, J. B., Rao, C. V., & Scokaert, P. O. M. (2000). Constrained model predictive control: Stability and optimality. *Automatica*, *36*(6), 789–814.

Mayne, D. Q., Seron, M. M., & Raković, S. V. (2005). Robust model predictive control of constrained linear systems with bounded disturbances. *Automatica*, *41*(2), 219–224.

Michalska, H., & Mayne, D. Q. (1993). Robust receding horizon control of constrained nonlinear systems. *IEEE Transactions on Automatic Control*, *38*(11), 1623–1633.

Mondada, F., Bonani, M., Raemy, X., Pugh, J., Cianci, C., & Klaptocz, A. et al. (2009). The e-puck, a robot designed for education in engineering. In *Proceedings of the 9th conference on autonomous robot systems and competitions* (pp. 59–65).

Narendra, P. M., & Fukunaga, K. (1977). A branch and bound algorithm for feature subset selection. *IEEE Transactions on Computers*, *26*(9), 917–922.

Rawlings, J. B., & Mayne, D. Q. (2009). *Model predictive control: Theory and design*. Nob Hill Pub..

Richards, A., & How, J. (2006). Robust stable model predictive control with constraint tightening. In *Proceedings of American control conference* (pp. 1557–1562).

Scokaert, P. O. M., & Rawlings, J. B. (1995). Stability of model predictive control under perturbations. In *Proceedings of the IFAC symposium on nonlinear control systems design* (pp. 1317–1322).

Shakouri, P., & Ordys, A. (2011). Application of the state-dependent nonlinear model predictive control in adaptive cruise control system. In *Proceedings of International IEEE conference on intelligent transportation systems* (pp. 686–691).

Shakouri, P., & Ordys, A. (2014). Nonlinear model predictive control approach in design of adaptive cruise control with automated switching to cruise control. *Control Engineering Practice*, *26*, 160–177.

Simanek, J., Reinstein, M., & Kubelka, V. (2015). Evaluation of the EKF-based estimation architectures for data fusion in mobile robots. *IEEE/ASME Transactions on Mechatronics*, *20*(2), 985–990.

Sontag, E. D. (2008). Input to state stability: Basic concepts and results. In *Nonlinear and optimal control theory* (pp. 163–220). Springer.

Sun, Z., & Xia, Y. (2016). Receding horizon tracking control of unicycle-type robots based on virtual structure. *International Journal of Robust and Nonlinear Control*, *26*(17), 3900–3918.

Tashiro, T. (2013). Vehicle steering control with MPC for target trajectory tracking of autonomous reverse parking. In *Proceedings of IEEE International conference on control applications* (pp. 247–251).

Wächter, A., & Biegler, L. T. (2006). On the implementation of an interior-point filter line-search algorithm for large-scale nonlinear programming. *Mathematical Programming*, *106*(1), 25–57.

Wan, Z., & Kothare, M. V. (2002). Robust output feedback model predictive control using off-line linear matrix inequalities. *Journal of Process Control*, *12*(7), 763–774.

Wang, P., & Ding, B. (2014). Distributed RHC for tracking and formation of nonholonomic multi-vehicle systems. *IEEE Transactions on Automatic Control*, *59*(6), 1439–1453.

Xia, Y. (2015). Cloud control systems. *IEEE/CAA Journal of Automatica Sinica*, *2*(2), 134–142.

Yang, J., & Kim, J. (1999). Sliding mode control for trajectory tracking of nonholonomic wheeled mobile robots. *IEEE Transactions on Robotics and Automation*, *15*(3), 578–587.

Yu, S., Maier, C., Chen, H., & Allgöwer, F. (2013). Tube MPC scheme based on robust control invariant set with application to lipschitz nonlinear systems. *Systems & Control Letters*, *62*(2), 194–200.

Zhang, X., Georghiou, A., & Lygeros, J. (2015). Convex approximation of chance-constrained MPC through piecewise affine policies using randomized and robust optimization. In *Proceedings of conference on decision and control* (pp. 3038–3043).

Zhongqi Sun was born in Hebei Province, China, in 1986. He received the B.S. degree in Computer and Automation in 2010 from Hebei Polytechnic University. He is now pursuing the Ph.D. degree in Control Science and Engineering in Beijing Institute of Technology. His research interests include multi-agent systems, model predictive control, nonlinear systems, and networked control systems.

Li Dai was born in Beijing, China, in 1988. She received the B.S. degree in Information and Computing Science in 2010 and the Ph.D. degree in Control Science and Engineering in 2016 from Beijing Institute of Technology, Beijing, China. Now she is an assistant professor in the School of Automation of Beijing Institute of Technology. Her research interests include model predictive control, distributed control, data-driven control, stochastic systems, and networked control systems.

Kun Liu received the Ph.D. degree in the Department of Electrical Engineering and Systems from Tel Aviv University, Tel Aviv, Israel, in December 2012. From February 2013 to February 2015 he was a postdoctoral researcher at the ACCESS Linnaeus Centre, KTH Royal Institute of Technology, Stockholm, Sweden. From March 2015 to August 2015 he held Researcher, Visiting, and Research Associate positions at, respectively, KTH Royal Institute of Technology, Stockholm, Sweden, CNRS, Laboratory for Analysis and Architecture of Systems, Toulouse, France, and The University of Hong Kong, Hong Kong. Since September 2015 he is an Associate Professor at the School of Automation, Beijing Institute of Technology, China. Currently he serves as Associate Editor in *IMA Journal of Mathematical Control and Information*. His research interests include networked control, time-delay systems, signal processing, and robust control.

Yuanqing Xia was born in Anhui Province, China, in 1971. He graduated from the Department of Mathematics, Chuzhou University, Chuzhou, China, in 1991. He received the M.S. degree in Fundamental Mathematics from Anhui University, Anhui, China, in 1998 and the Ph.D. degree in Control Theory and Control Engineering from the Beijing University of Aeronautics and Astronautics, Beijing, China, in 2001. From 1991 to 1995, he was with Tongcheng Middle-School, Anhui, where he worked as a Teacher. During January 2002–November 2003, he was a Postdoctoral Research Associate with the Institute of Systems Science, Academy of Mathematics and System Sciences, Chinese Academy of Sciences, Beijing, China, where he worked on navigation, guidance and control. From November 2003 to February 2004, he was with the National University of Singapore as a Research Fellow, where he worked on variable structure control. From February 2004 to February 2006, he was with the University of Glamorgan, Pontypridd, UK, as a Research Fellow, where he worked on networked control systems. From February 2007 to June 2008, he was a Guest Professor with Innsbruck Medical University, Innsbruck, Austria, where he worked on biomedical signal processing. Since 2004, he has been with the Department of Automatic Control, Beijing Institute of Technology, Beijing, first as an Associate Professor, then, since 2008, as a Professor. In 2012, he was appointed as Xu Teli Distinguished Professor at the Beijing Institute of Technology and obtained a National Science Foundation for Distinguished Young Scholars of China. His current research interests are in the fields of networked control systems, robust control and signal processing, active disturbance rejection control and flight control. He has published eight monographs with Springer and Wiley, and more than 100 papers in journals. He has obtained Second Award of the Beijing Municipal Science and Technology (No. 1) in 2010, Second National Award for Science and Technology (No. 2) in 2011, and Second Natural Science Award of The Ministry of Education (No. 1) in 2012. He is a Deputy Editor of the Journal of the Beijing Institute of Technology, Associate Editor of Acta Automatica Sinica, Control Theory and Applications, the International Journal of Innovative Computing, Information and Control, and the International Journal of Automation and Computing.

Karl Henrik Johansson is Director of the Stockholm Strategic Research Area ICT The Next Generation and Professor at the School of Electrical Engineering, KTH Royal Institute of Technology. He received M.Sc. and Ph.D. degrees in Electrical Engineering from Lund University. He has held visiting positions at UC Berkeley, Caltech, NTU, HKUST Institute of Advanced Studies, and NTNU. His research interests are in networked control systems, cyber–physical systems, and applications in transportation, energy, and automation. He is a member of the IEEE Control Systems Society Board of Governors and the European Control Association Council. He has received several best paper awards and other distinctions, including a ten-year Wallenberg Scholar Grant, a Senior Researcher Position with the Swedish Research Council, the Future Research Leader Award from the Swedish Foundation for Strategic Research, and the triennial Young Author Prize from IFAC. He is member of the Royal Swedish Academy of Engineering Sciences, Fellow of the IEEE, and IEEE Distinguished Lecturer.